Electronic Supplementary Material (ESI) for Physical Chemistry Chemical Physics.

A Computational Study of Electronic Circular Dichroism Spectra of Single-Chain Transoid and Cisoid Oligothiophenes in Chiral Conformation.

Electronic Supplementary Information

Daniel Aranda[a,b], Javier Cerezo[c], Gennaro Pescitelli[d], Francisco J. Avila Ferrer[a], Juan Soto[a], Fabrizio Santoro[b]*

[a].*Department of Physical Chemistry, Faculty of Science, University of Málaga, E-29071-Málaga, Spain.*

[b] *Consiglio Nazionale delle Ricerche – CNR, Istituto di Chimica dei Composti Organo Metallici (ICCOM-CNR), UOS di Pisa, Via G. Moruzzi 1, I-56124 Pisa, Italy†. E-mail:fabrizio.santoro@pi.iccom.cnr.it*

[c] *Department of Physical Chemistry, Faculty of Chemistry, University of Murcia, E-30100-Murcia, Spain.*

[d] *Università di Pisa, Dipartimento di Chimica e Chimica Industriale Via G. Moruzzi, 13, I-56124 Pisa, Italy.*

Table S1a. Oscillator strength (OS), vertical energy (VE) and rotatory strength (RS) for the three first excited states of transoid T_{13} at θ=15º with different basis sets.

	S1			S2			S3		
	OS	VE (eV)	RS (10^{-40} cgs)	OS	VE (eV)	RS (10^{-40} cgs)	OS	VE (eV)	RS (10^{-40} cgs)
6-31G(d)	4.9906	2.7657	338	0.0000	3.0409	0	0.3856	3.3382	29
6-311G(d,p)	4.8447	2.7309	340	0.0000	2.9959	0	0.3707	3.2803	29
6-311+G(2d,p)	4.6701	2.6755	380	0.0000	2.929	0	0.3469	3.1974	32
6-311+G(2d,2p)	4.6621	2.6739	381	0.0000	2.9272	0	0.3464	3.1954	32

Table S1b. Oscillator strength (OS), vertical energy (VE) and rotatory strength (RS) for the three first excited states of cisoid T_{13} at θ=15º with different basis sets.

	S1			S2			S3		
	OS	VE (eV)	RS (10^{-40} cgs)	OS	VE (eV)	RS (10^{-40} cgs)	OS	VE (eV)	RS (10^{-40} cgs)
6-31G(d)	1.3158	2.6940	8011	1.8776	2.9922	-9400	1.7222	3.3247	591
6-311G(d,p)	1.2810	2.6574	7831	1.8125	2.9479	-9114	1.6555	3.2711	579
6-311+G(2d,p)	1.2265	2.6070	7642	1.7031	2.8857	-8750	1.5319	3.1926	481
6-311+G(2d,2p)	1.2246	2.6055	7629	1.7011	2.8839	-8715	1.5304	3.1905	482

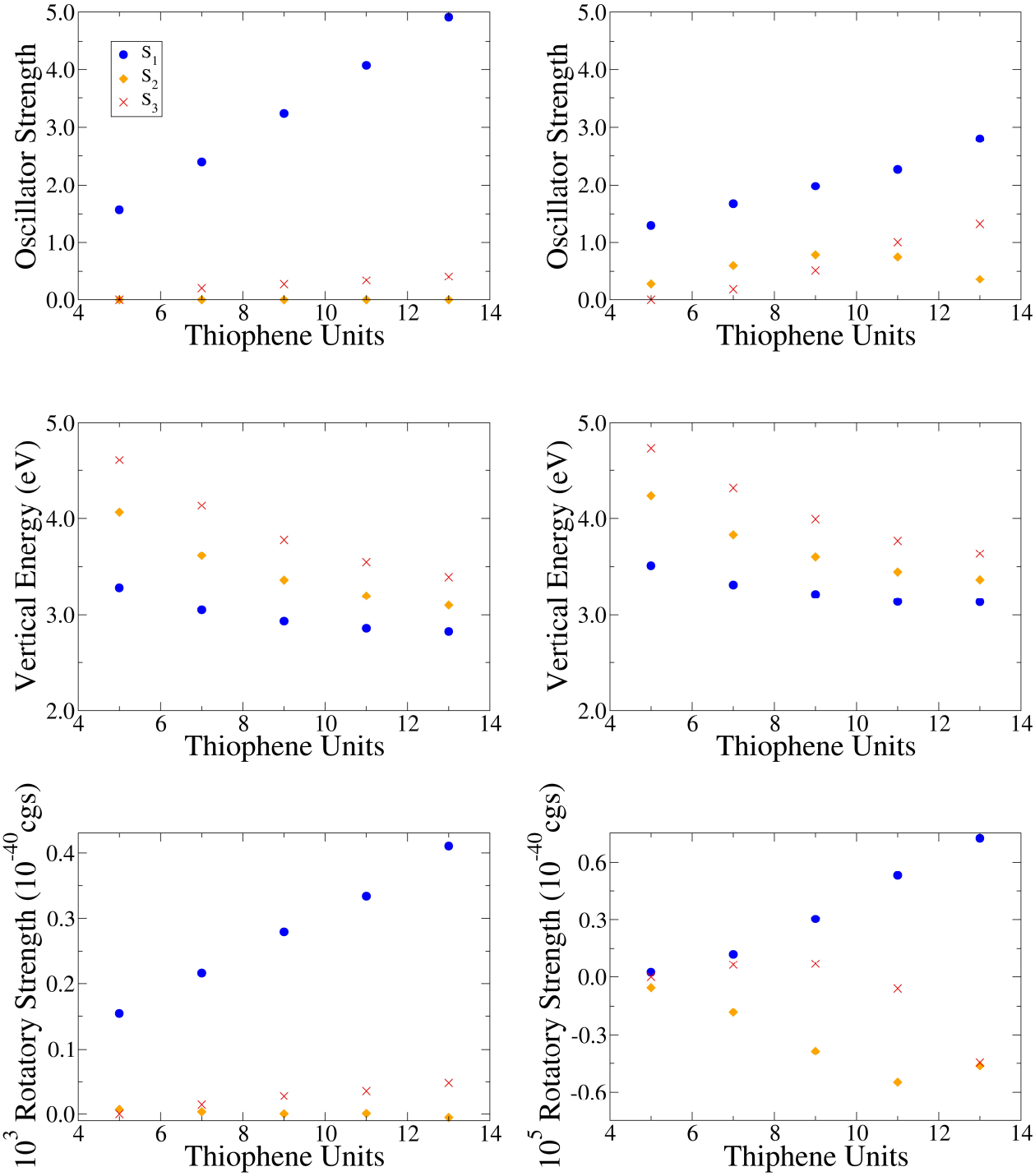

Figure S1. Oscillator Strength (top), Vertical Transition Energy (middle) and Rotatory Strength (bottom) dependence with the number of thiophene units for the all-trans (left) and all-cis (right) molecules of class *I*.

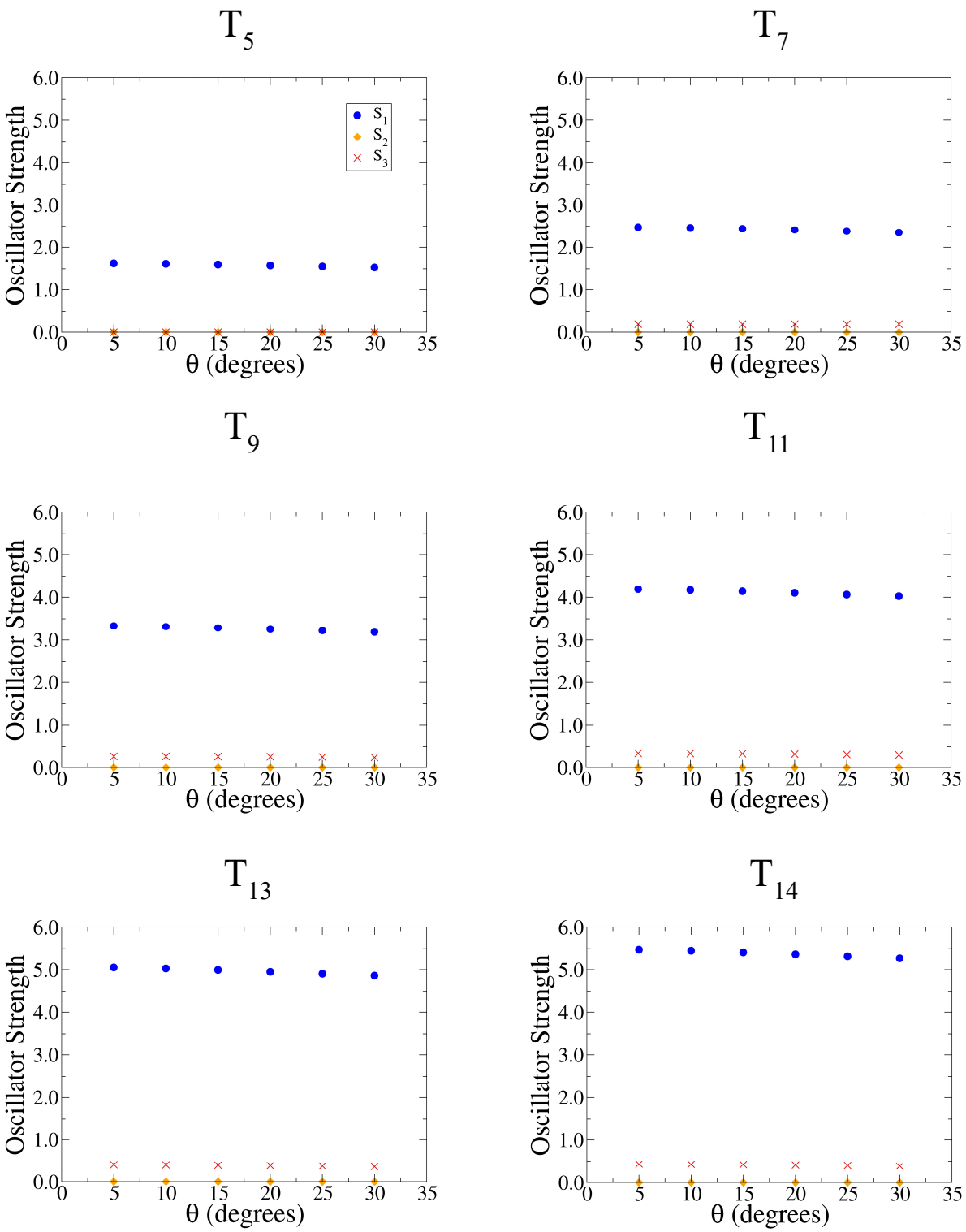

Figure S2. Oscillator Strength dependence with θ for S_1, S_2 and S_3 of the all-trans molecules of class *II*.

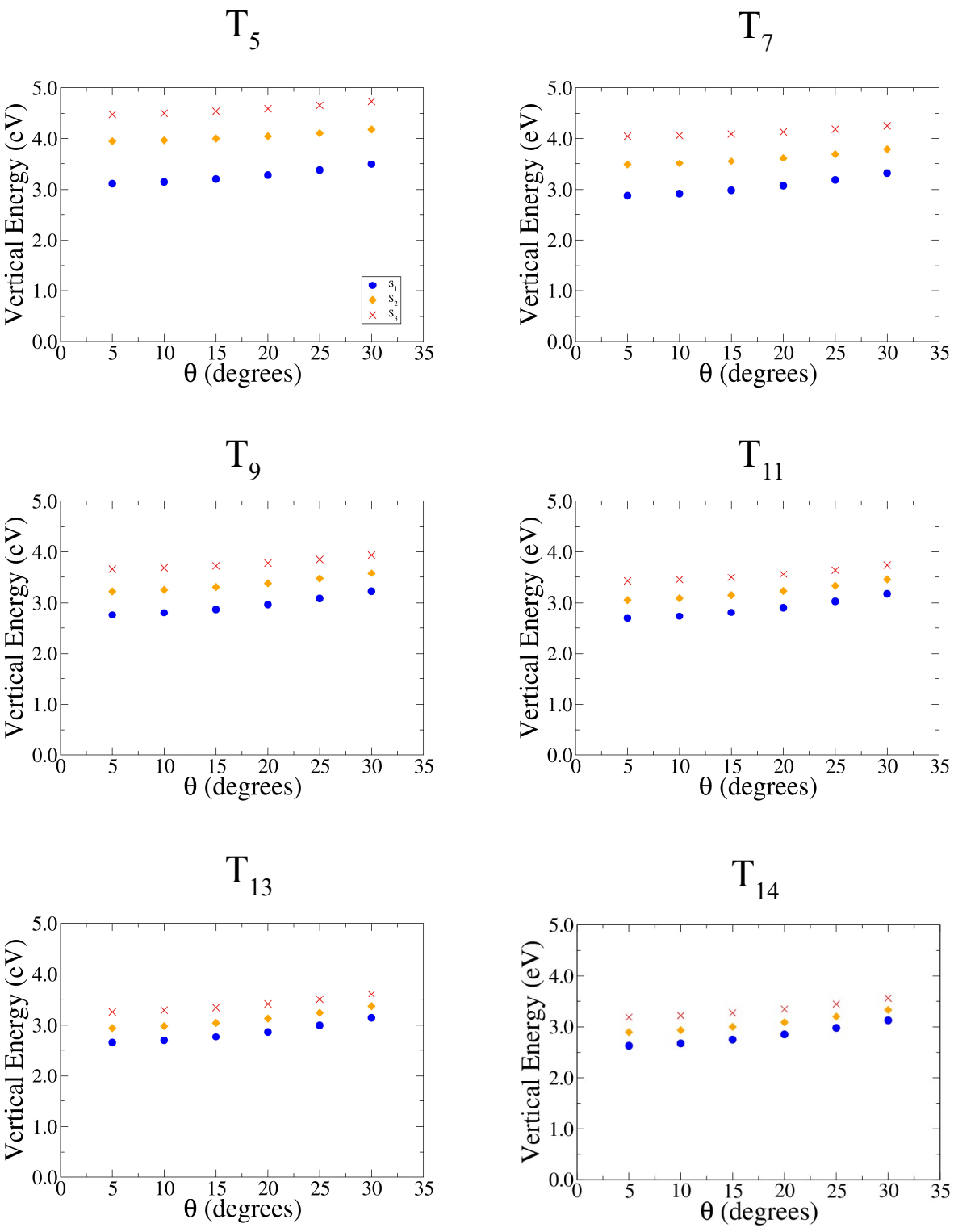

Figure S3. Vertical Transition Energy dependence with θ for S_1, S_2 and S_3 of the all-trans molecules of class *II*.

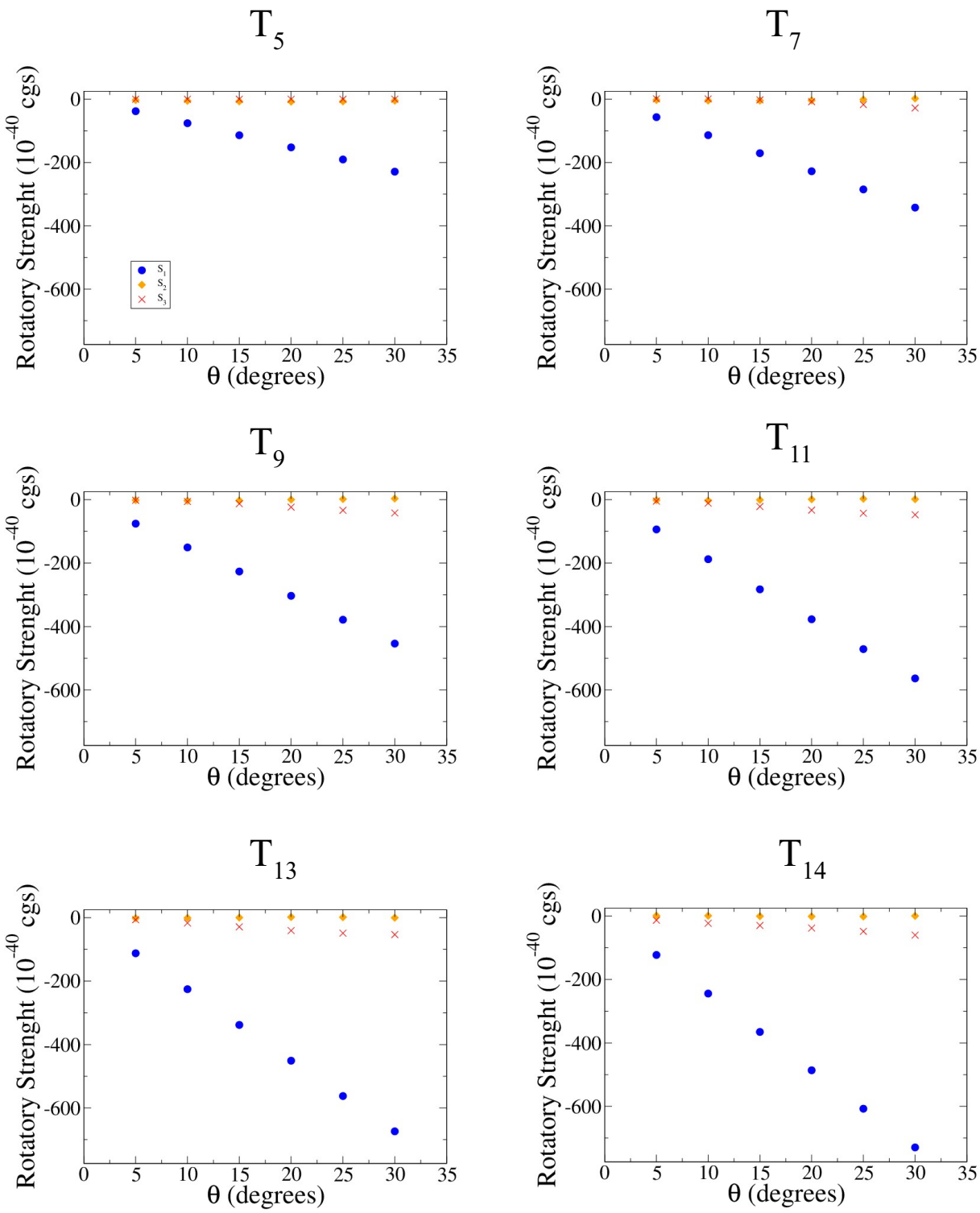

Figure S4. Rotatory Strength dependence with θ for S_1, S_2 and S_3 of the all-trans molecules of class *II*.

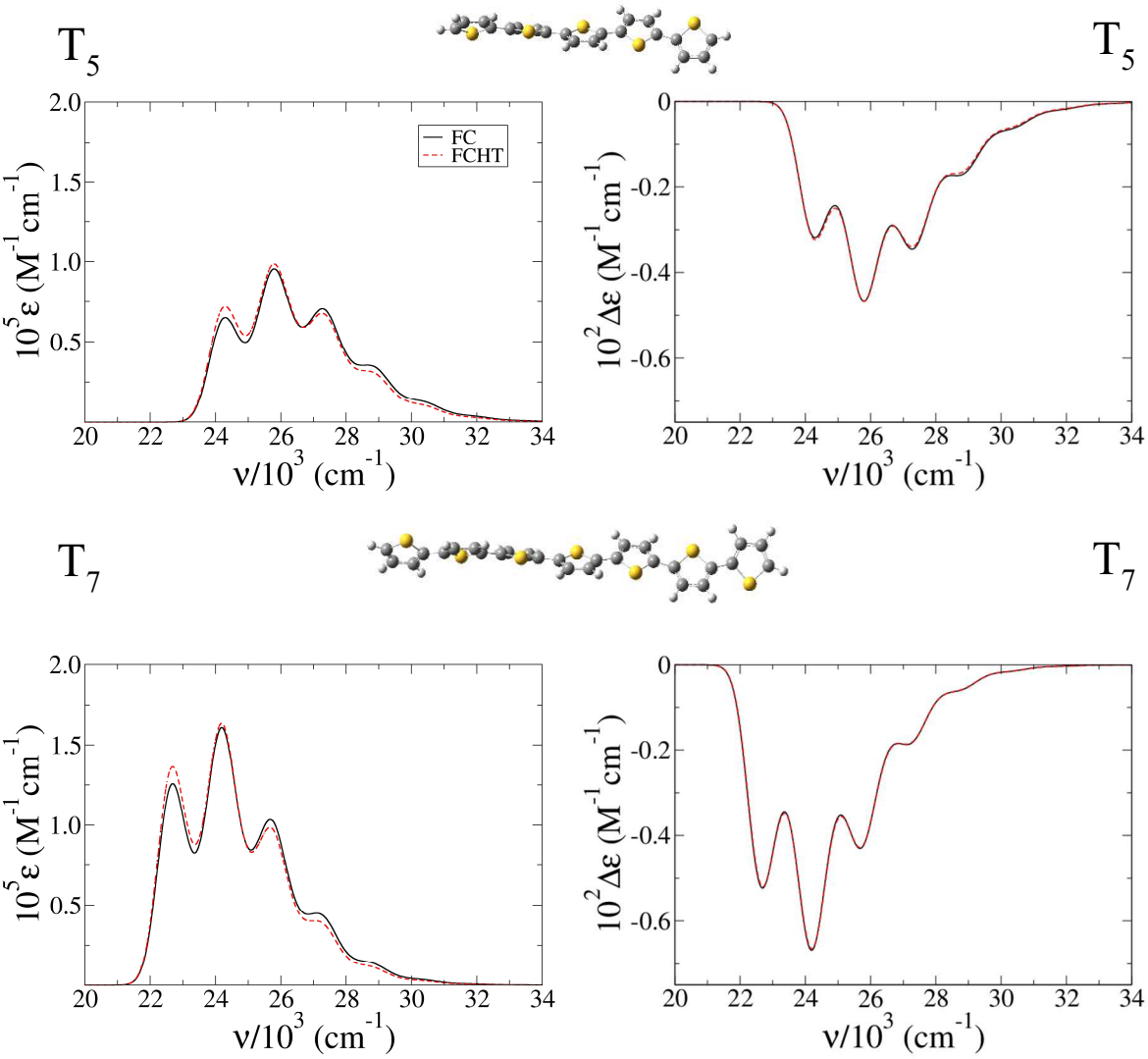

Figure S5. FC and FCHT absorption (left) and ECD (right) spectra computed for the *class I* structure of T_5, and T_7 transoid twisted ribbons at 0K and broadened with a Gaussian with HWHM=450 cm^{-1}. Inter-ring torsion angles are considered frozen during the transition.

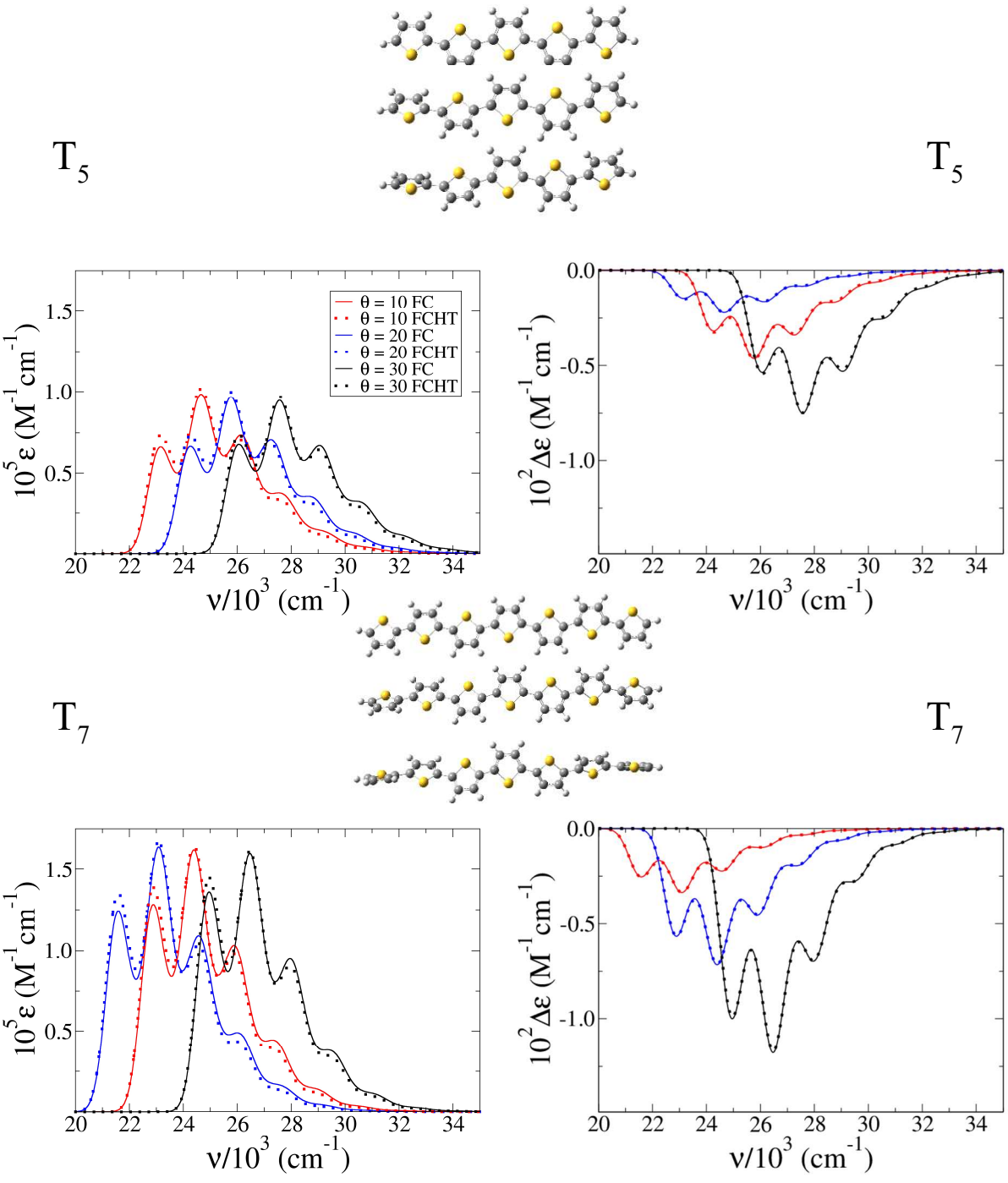

Figure S6. FC absorption (left) and ECD (right) spectra computed for the *class II* structure of T_5, and T_7 transoid twisted ribbons at 0K and broadened with a Gaussian with HWHM=450 cm^{-1} at different torsion angles (considered frozen during the transition).

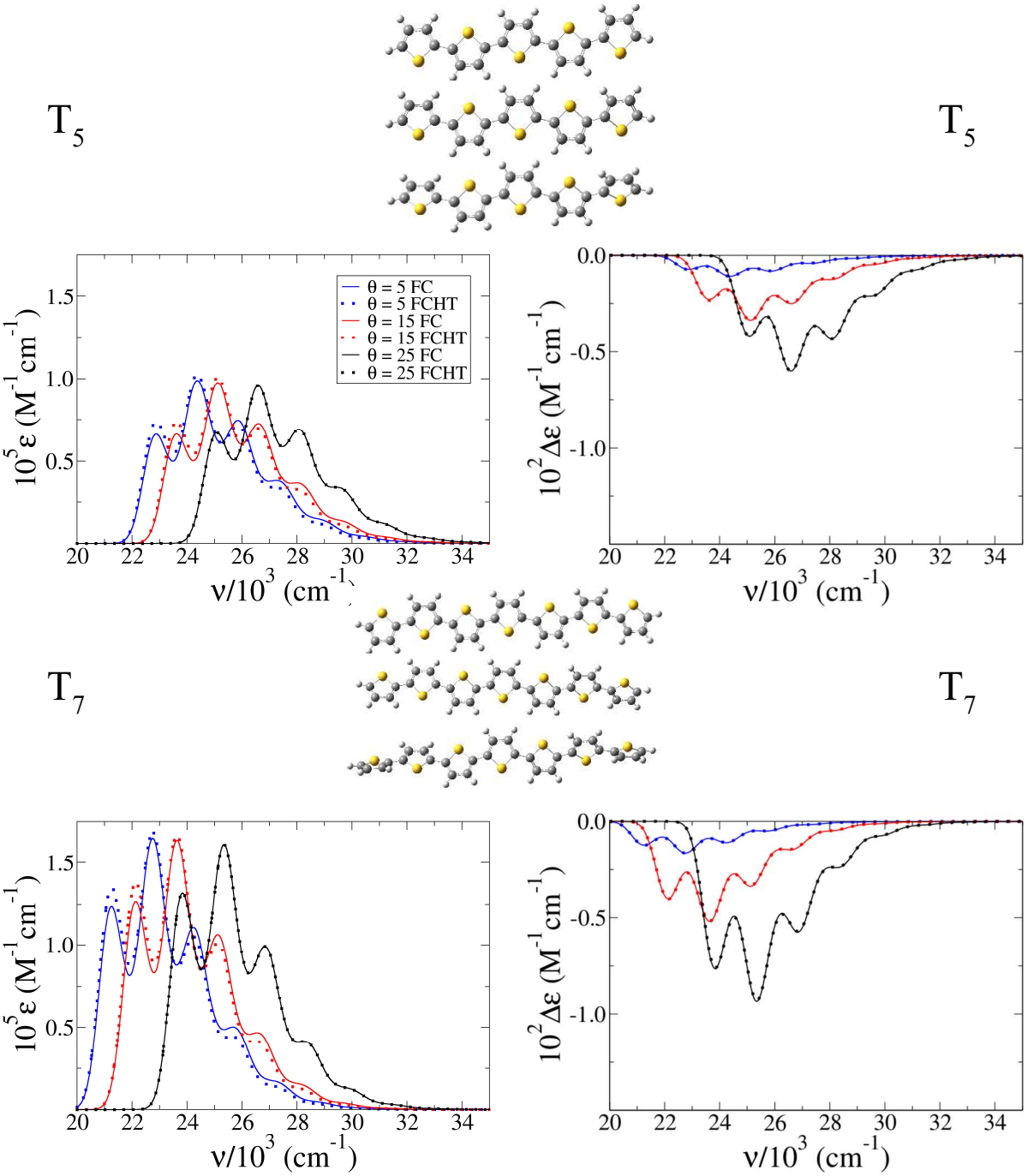

Figure S7. FC absorption (left) and ECD (right) spectra computed for the *class II* structure of T_5, and T_7 transoid twisted ribbons at 0K and broadened with a Gaussian with HWHM=450 cm^{-1} at different torsion angles (considered frozen during the transition).

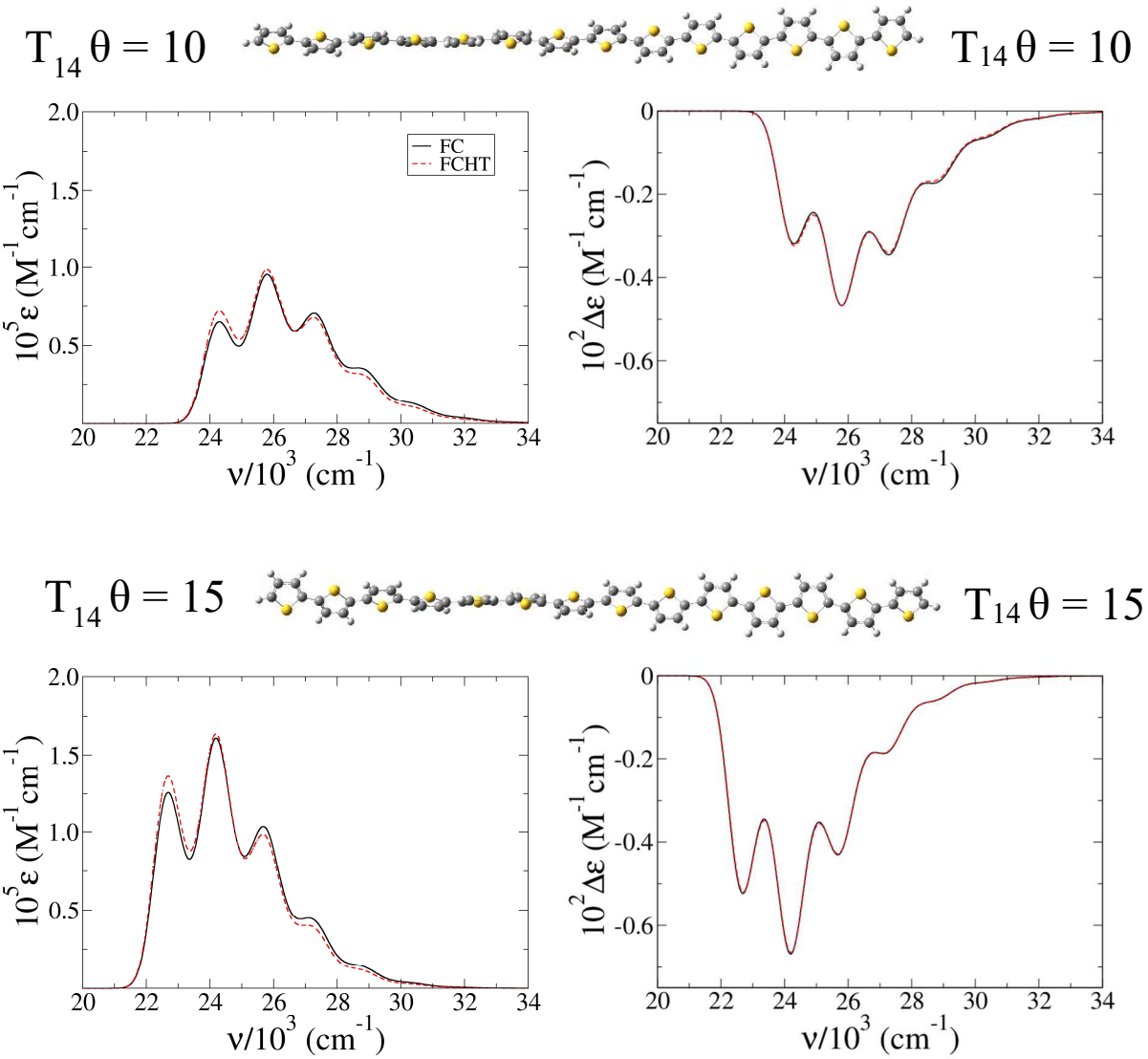

Figure S8. FC and FCHT absorption (left) and ECD (right) spectra computed for the *class II* structure of T_{14} with θ = 10 (top) and θ = 15 (bottom) transoid twisted ribbons at 0K and broadened with a Gaussian with HWHM=450 cm^{-1}. Inter-ring torsion angles are considered frozen during the transition.

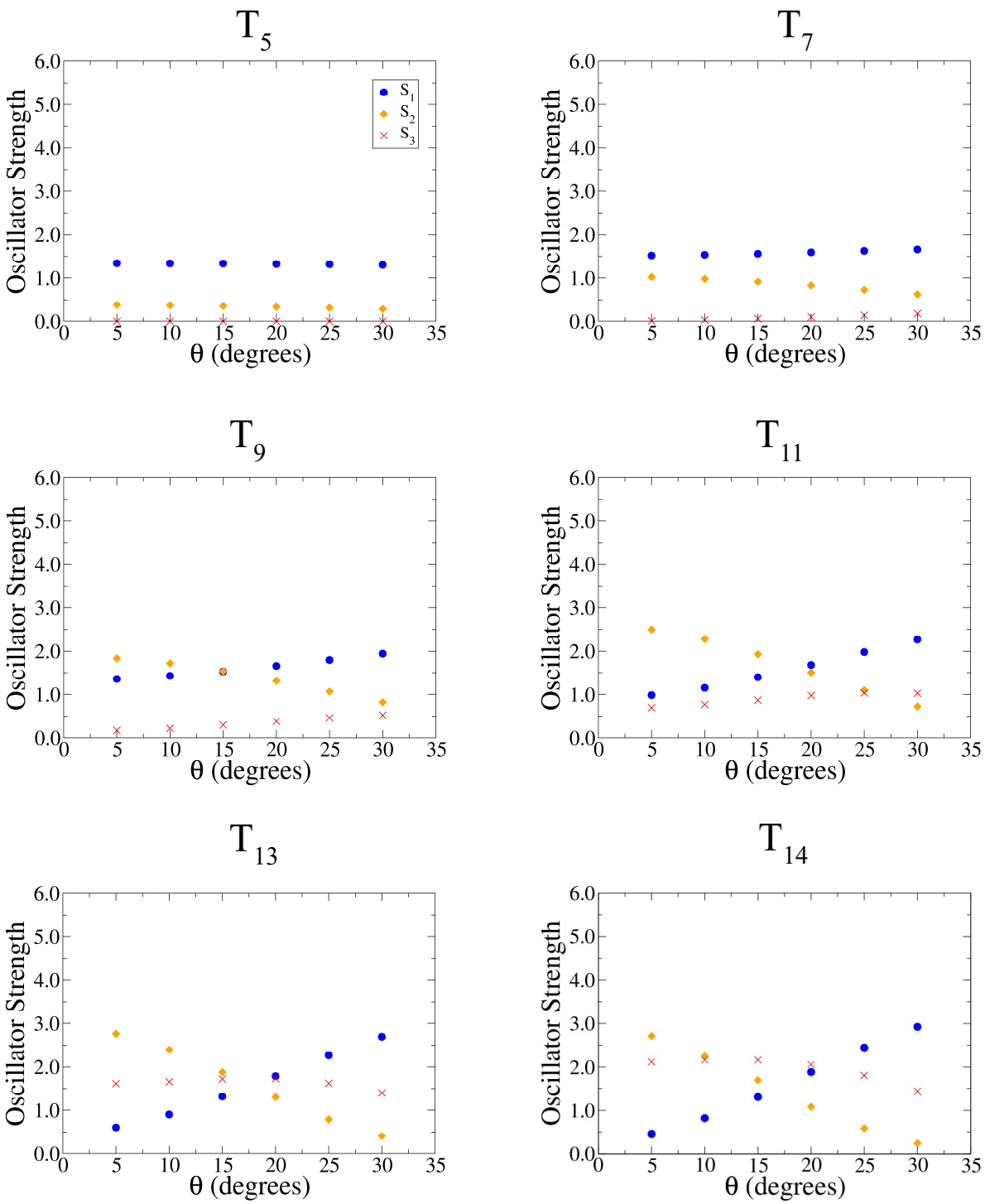

Figure S9. Oscillator Strength dependence with θ for S_1, S_2 and S_3 of the all-cis molecules of class *II*.

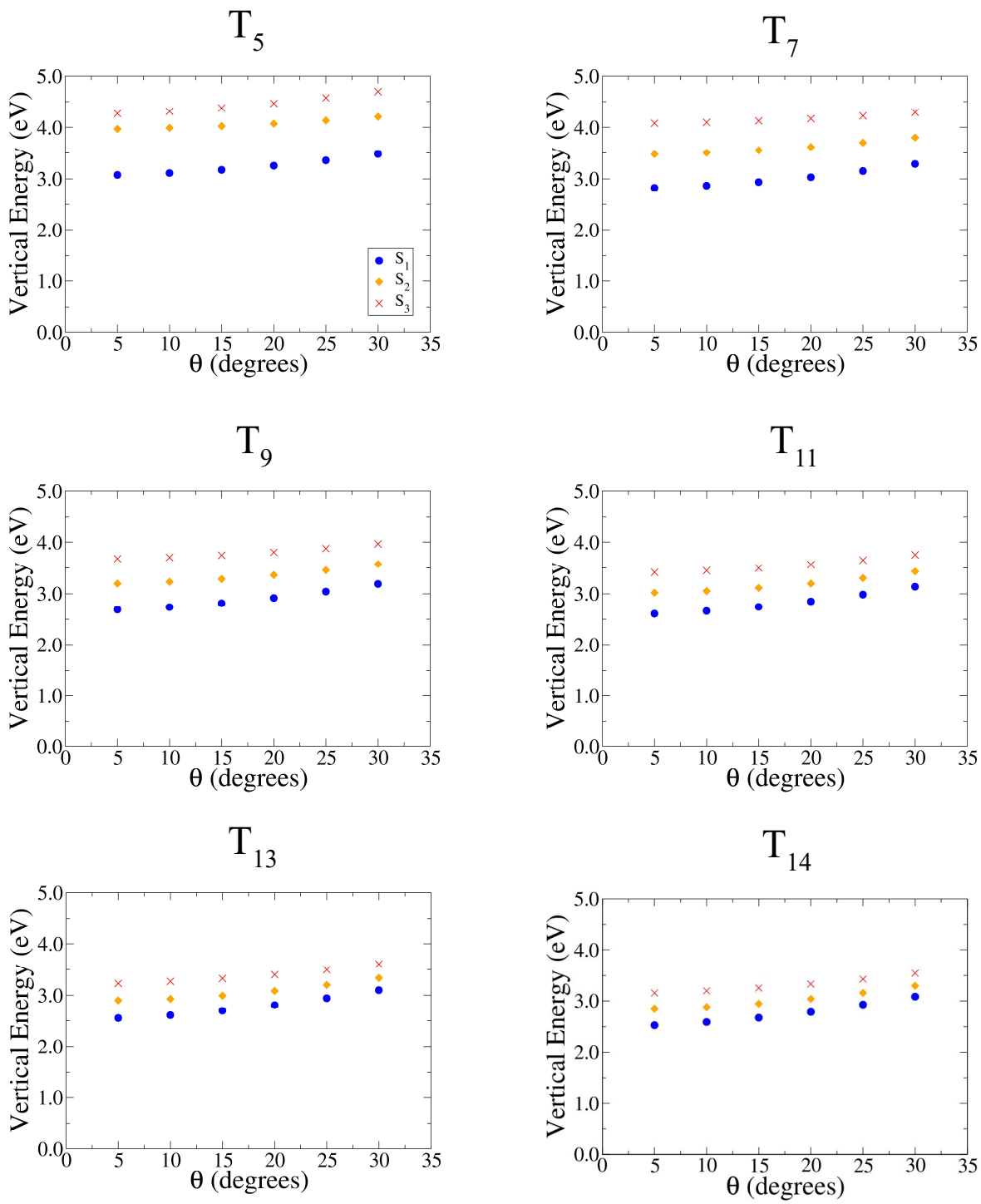

Figure S10. Vertical Transition Energy dependence with θ for S_1, S_2 and S_3 of the all-cis molecules of class *II*.

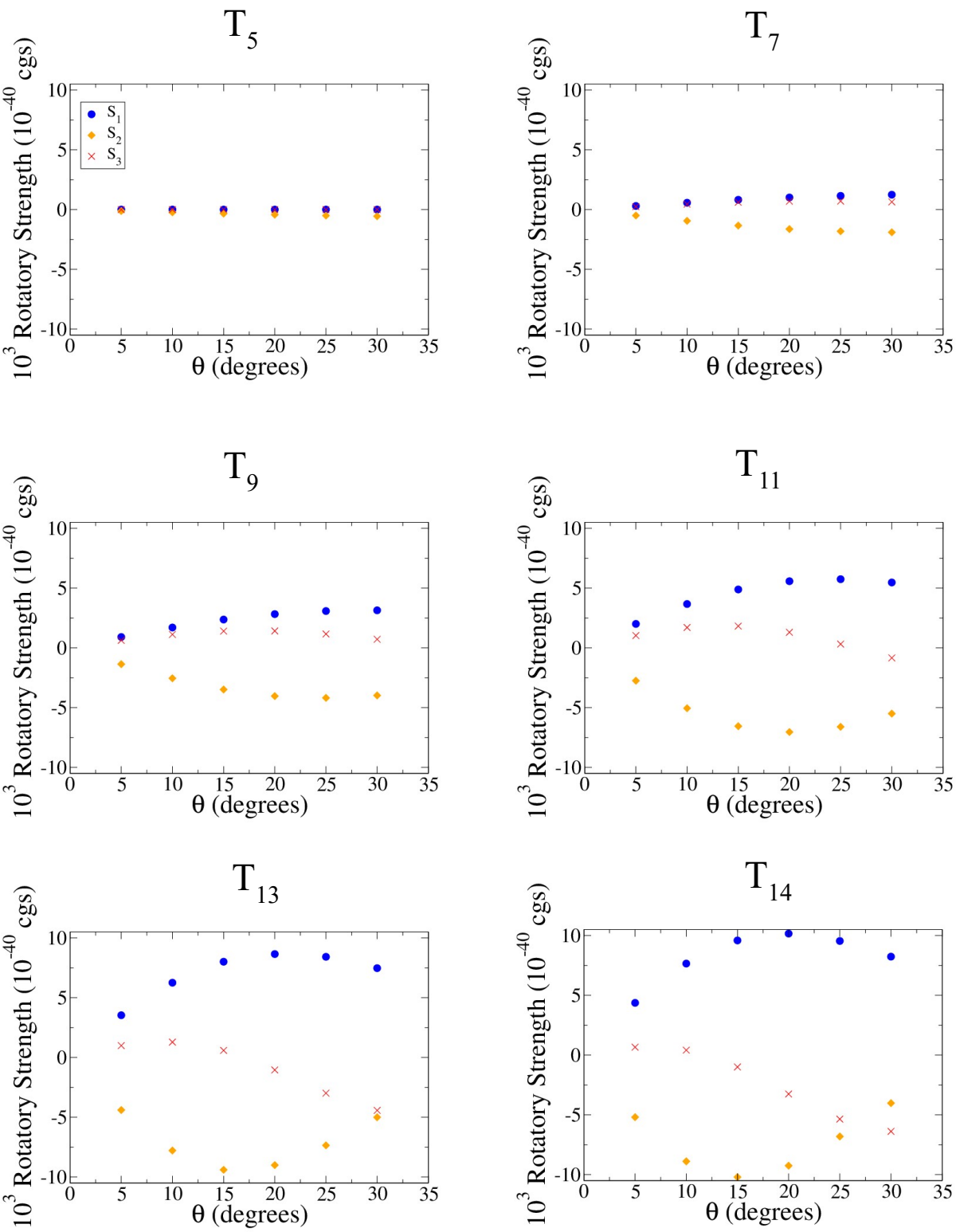

Figure S11. Rotatory Strength dependence with θ for S_1, S_2 and S_3 of the all-cis molecules of class *II*.

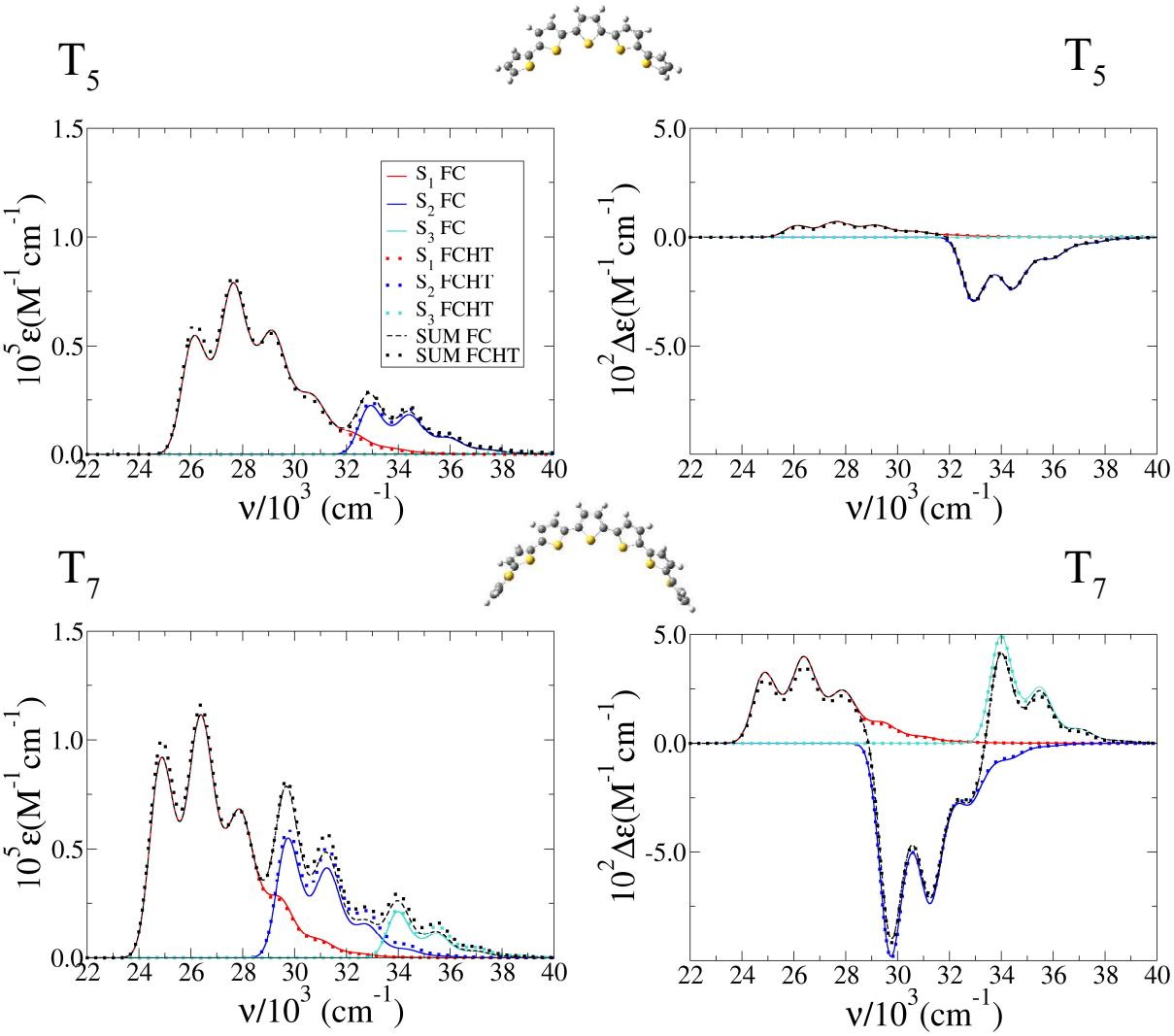

Figure S12. FC and FCHT absorption (left) and ECD (right) spectra computed for the *class I* structure of T_5, and T_7 transoid twisted ribbons at 0K and broadened with a Gaussian with HWHM=450 cm^{-1}. Inter-ring torsion angles are considered frozen during the transition.

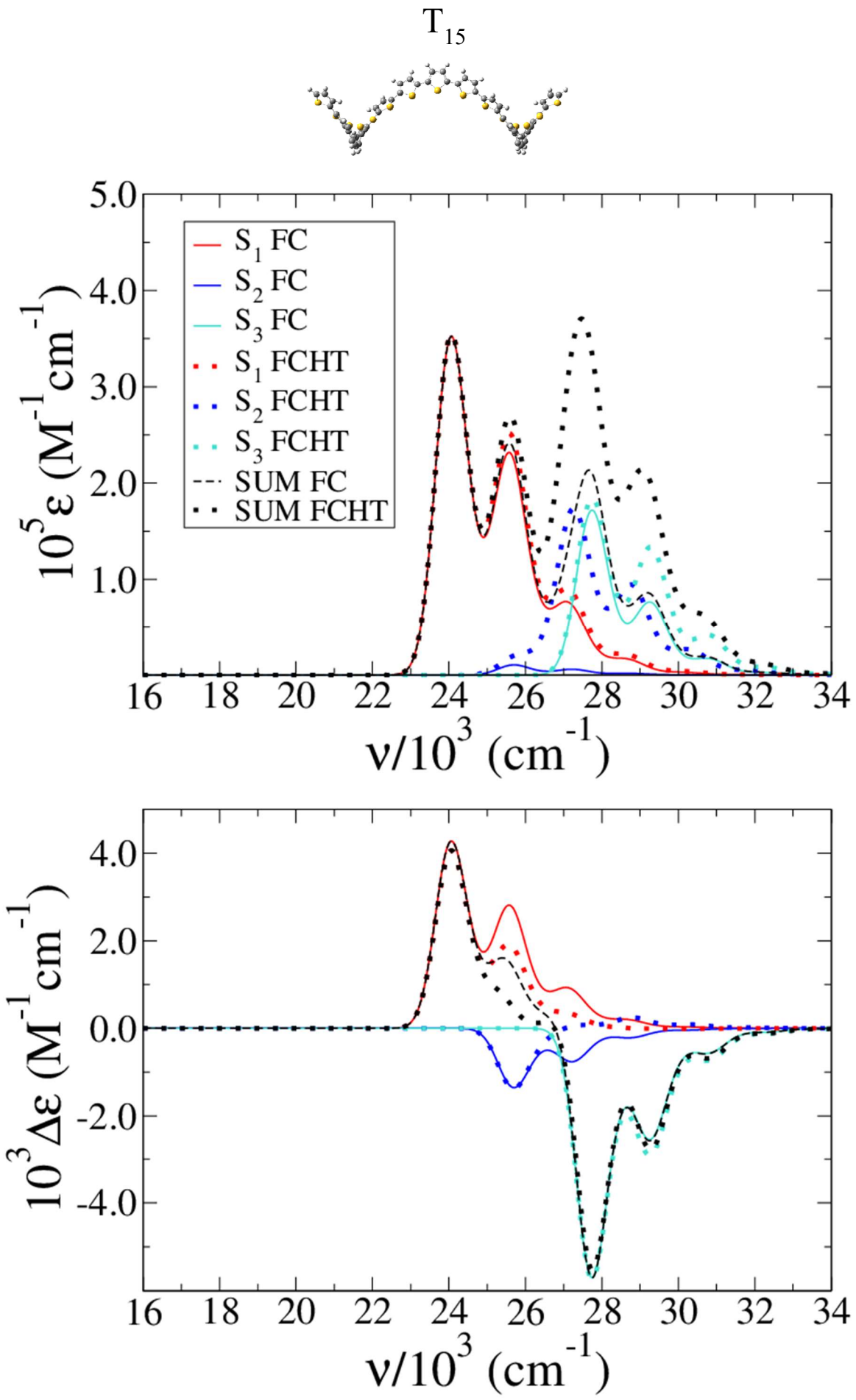

Figure S13. FC and FCHT absorption (top) and ECD (bottom) spectra computed for the *class I* structure of T_{15} cisoid helix at 0K and broadened with a Gaussian with HWHM=450 cm^{-1}. Inter-ring torsion angles are considered frozen during the transition.

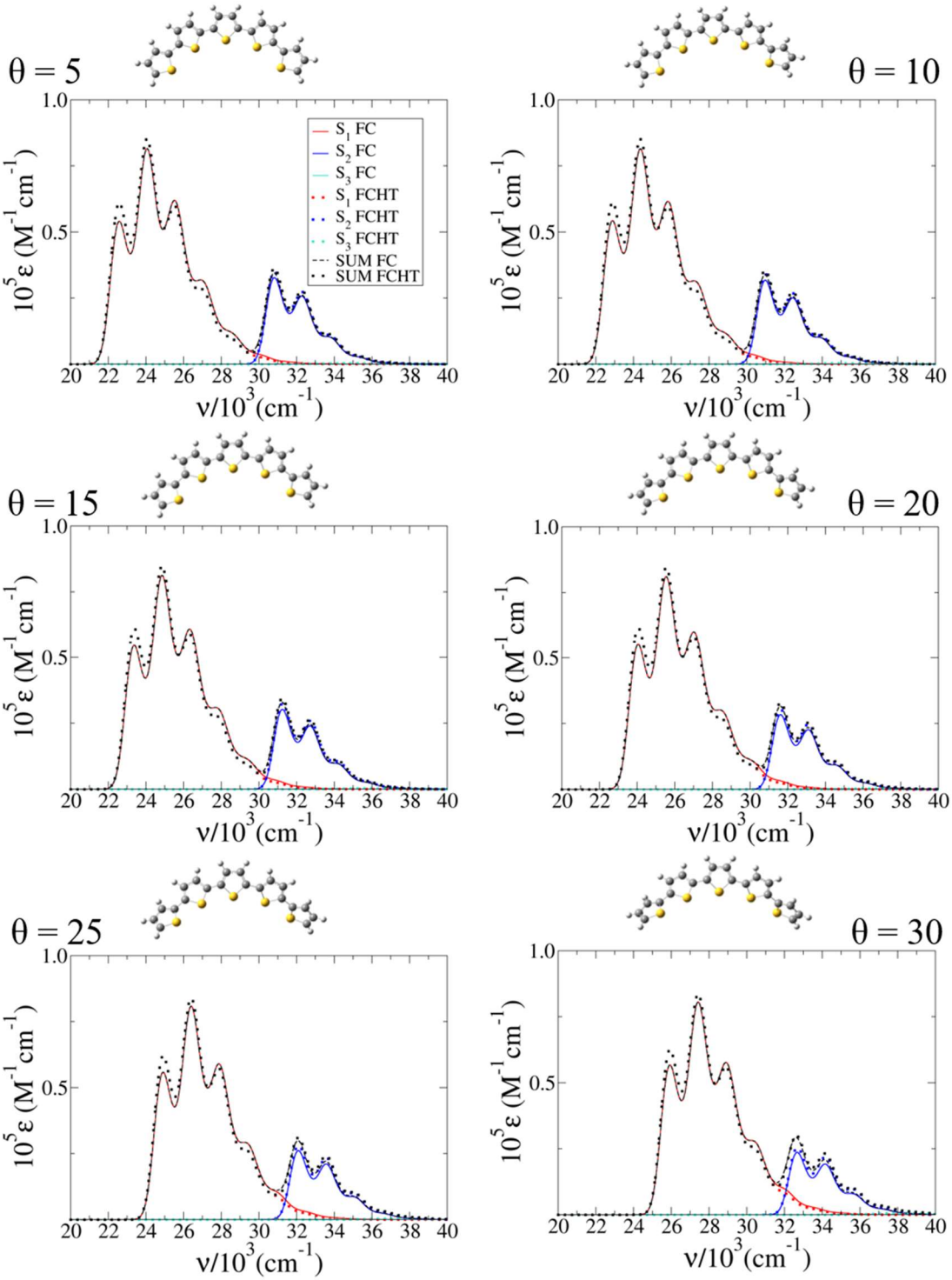

Figure S14. FC and FCHT contribution of S1, S2 and S3 to the absorption spectra computed for the *class II* structure of T_5 cisoid helices at 0K and broadened with a Gaussian with HWHM=450 cm^{-1} at different torsion angles (considered frozen during the transition).

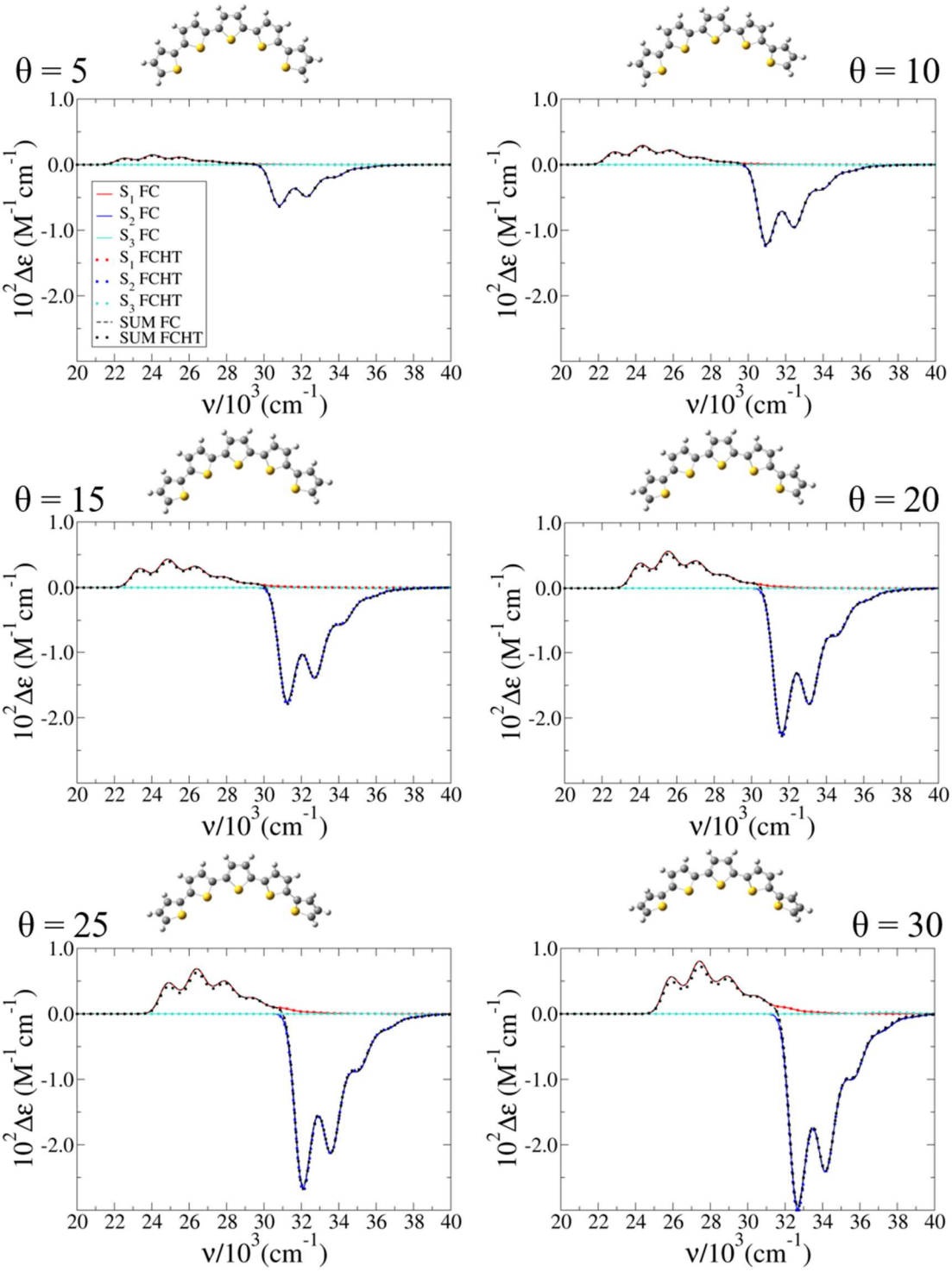

Figure S15. FC and FCHT contribution of S1, S2 and S3 to the ECD spectra computed for the *class II* structure of T_5 cisoid helices at 0K and broadened with a Gaussian with HWHM=450 cm^{-1} at different torsion angles (considered frozen during the transition).

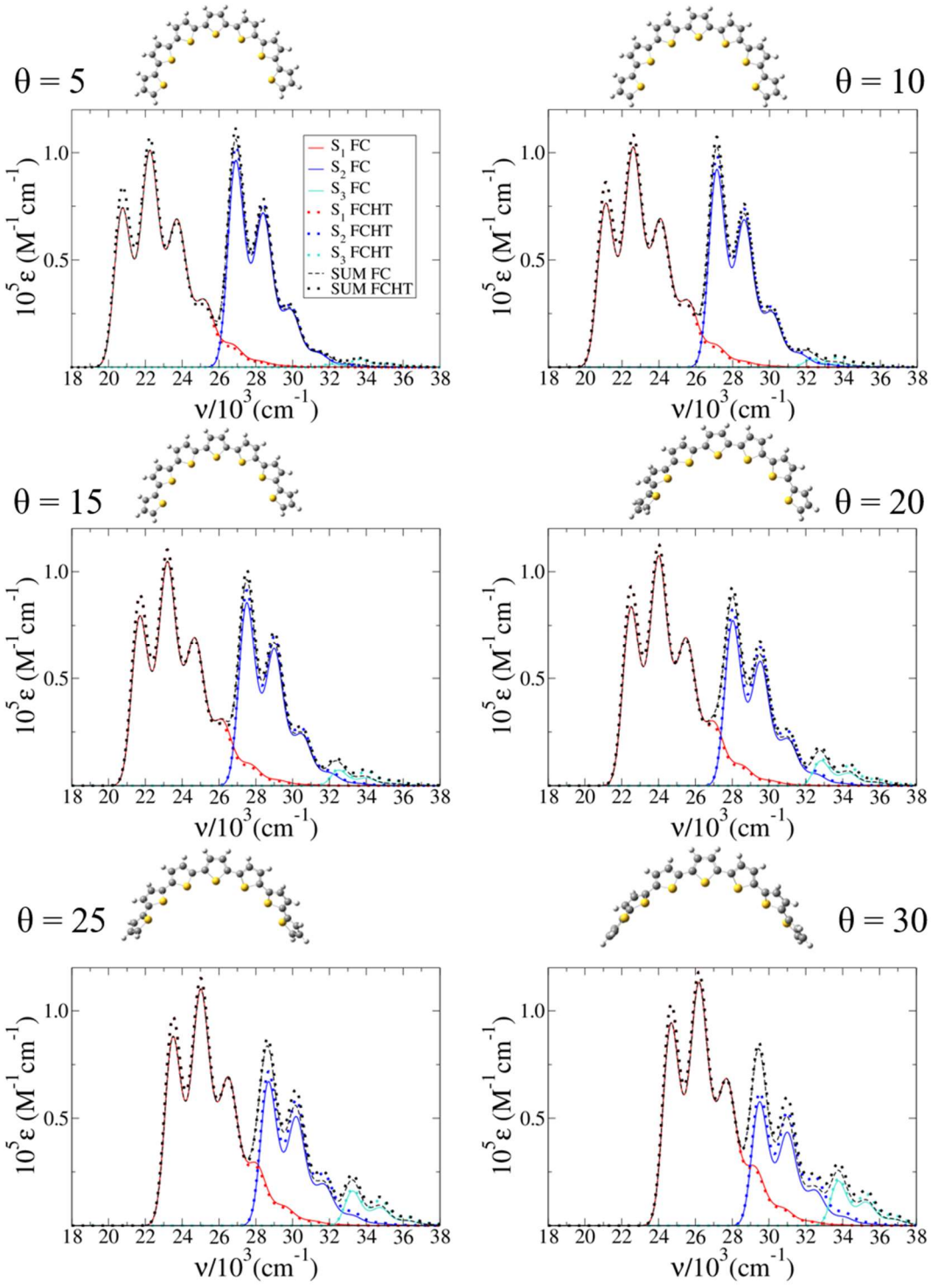

Figure S16. FC and FCHT contribution of S1, S2 and S3 to the absorption spectra computed for the *class II* structure of T_7 cisoid helices at 0K and broadened with a Gaussian with HWHM=450 cm^{-1} at different torsion angles (considered frozen during the transition).

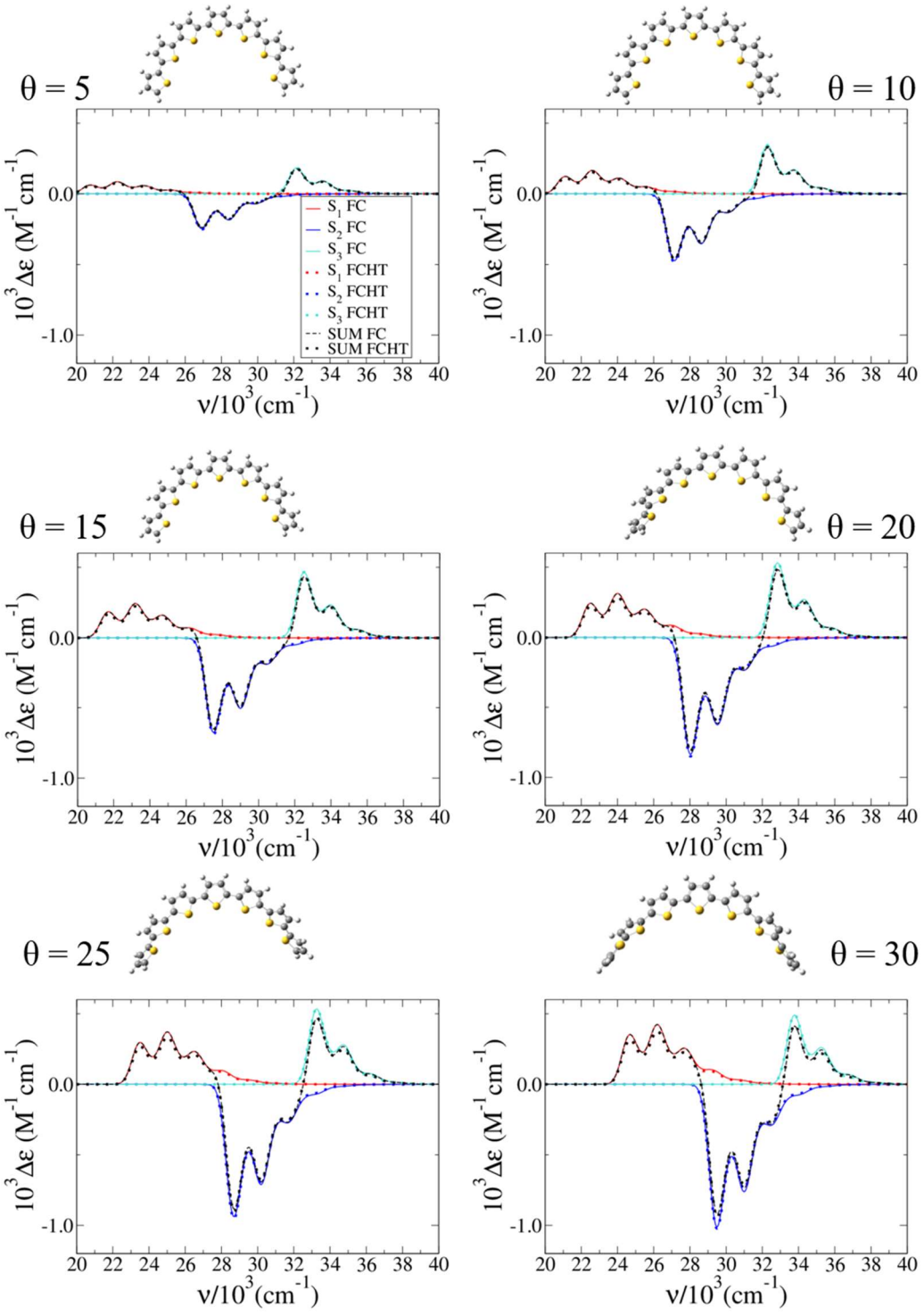

Figure S17. FC and FCHT contribution of S1, S2 and S3 to the ECD spectra computed for the *class II* structure of T_7 cisoid helices at 0K and broadened with a Gaussian with HWHM=450 cm^{-1} at different torsion angles (considered frozen during the transition).

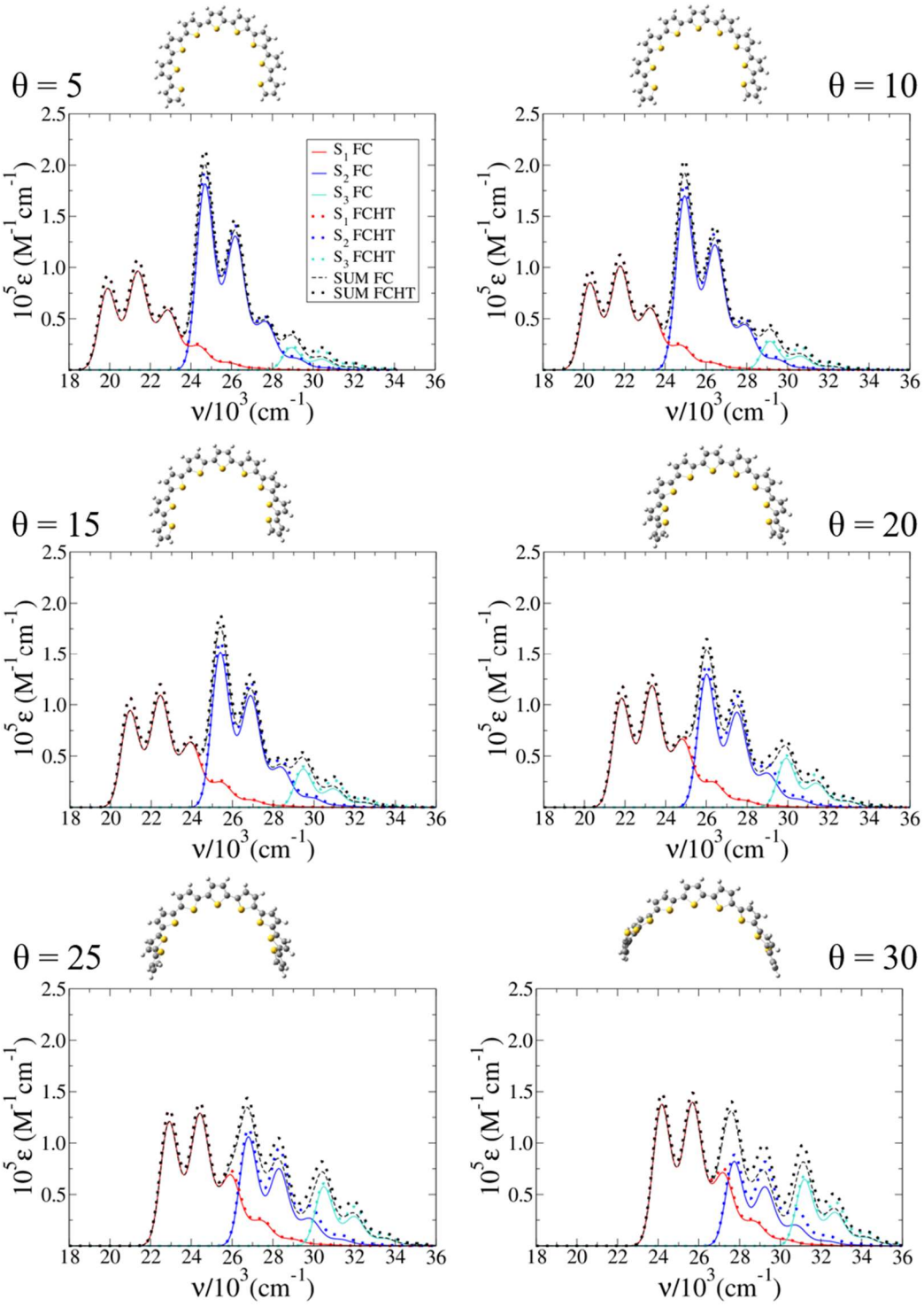

Figure S18. FC and FCHT contribution of S1, S2 and S3 to the absorption spectra computed for the *class II* structure of T_9 cisoid helices at 0K and broadened with a Gaussian with HWHM=450 cm^{-1} at different torsion angles (considered frozen during the transition).

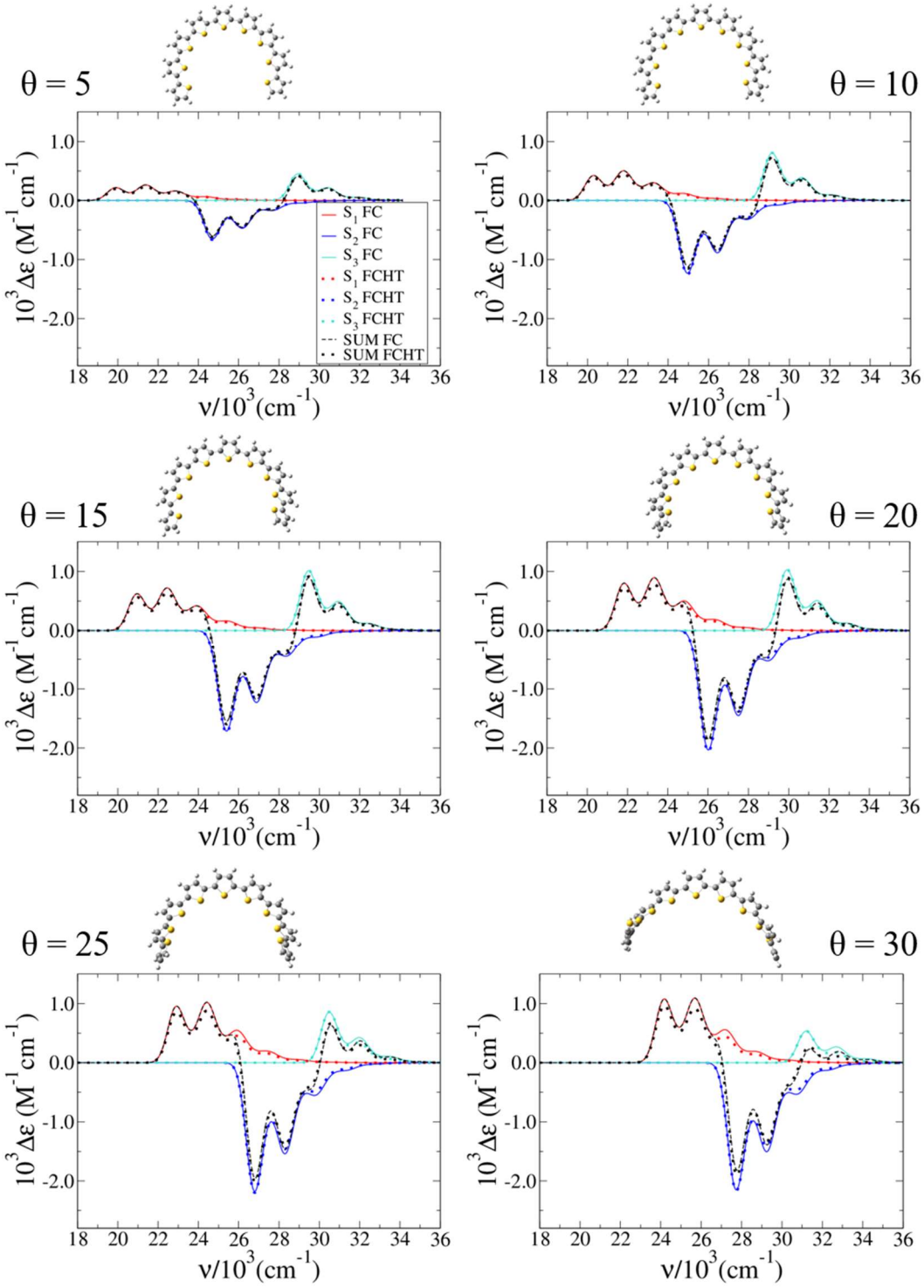

Figure S19. FC and FCHT contribution of S1, S2 and S3 to the ECD spectra computed for the *class II* structure of T_9 cisoid helices at 0K and broadened with a Gaussian with HWHM=450 cm^{-1} at different torsion angles (considered frozen during the transition).

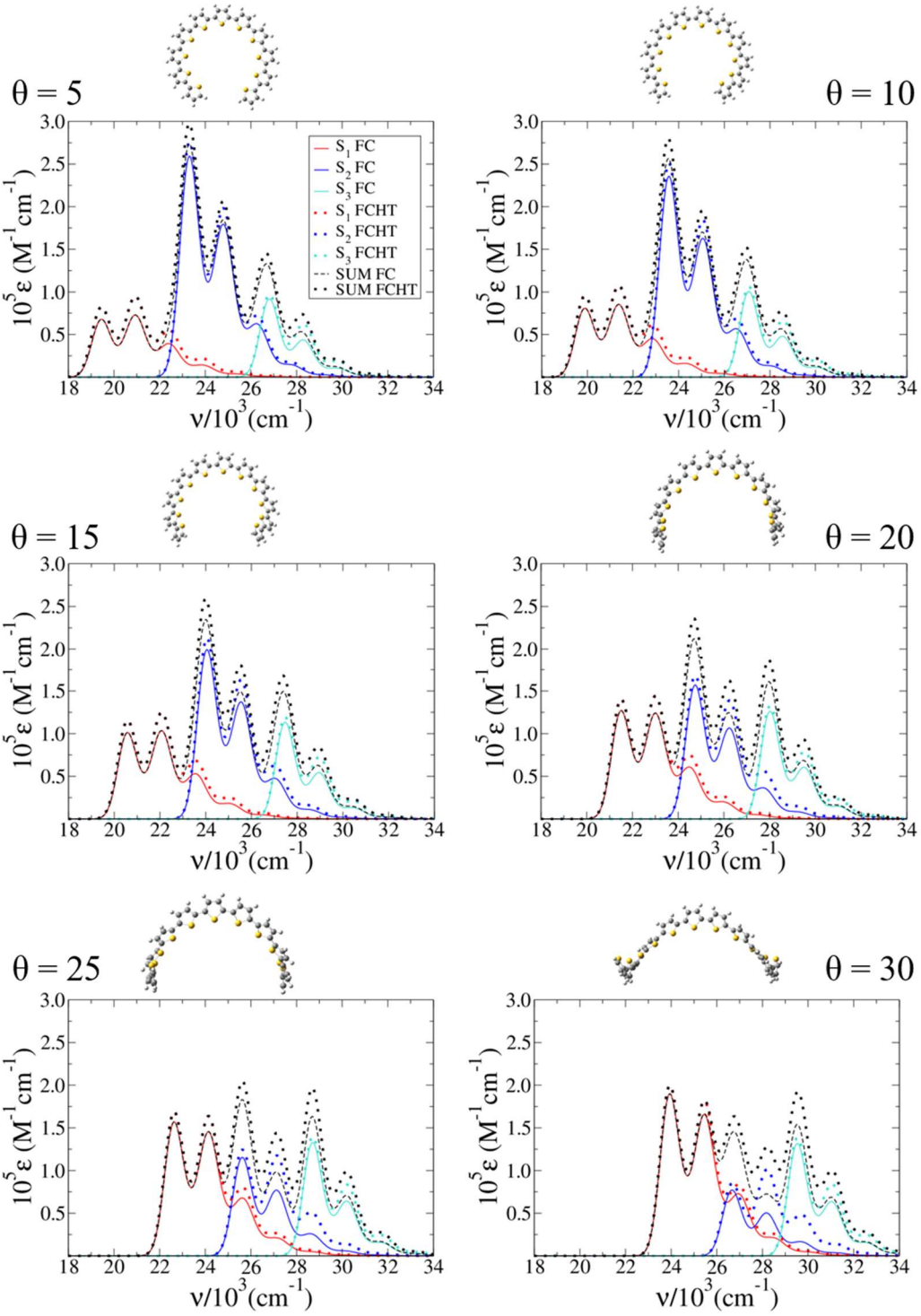

Figure S20. FC and FCHT contribution of S1, S2 and S3 to the absorption spectra computed for the *class II* structure of T_{11} cisoid helices at 0K and broadened with a Gaussian with HWHM=450 cm^{-1} at different torsion angles (considered frozen during the transition).

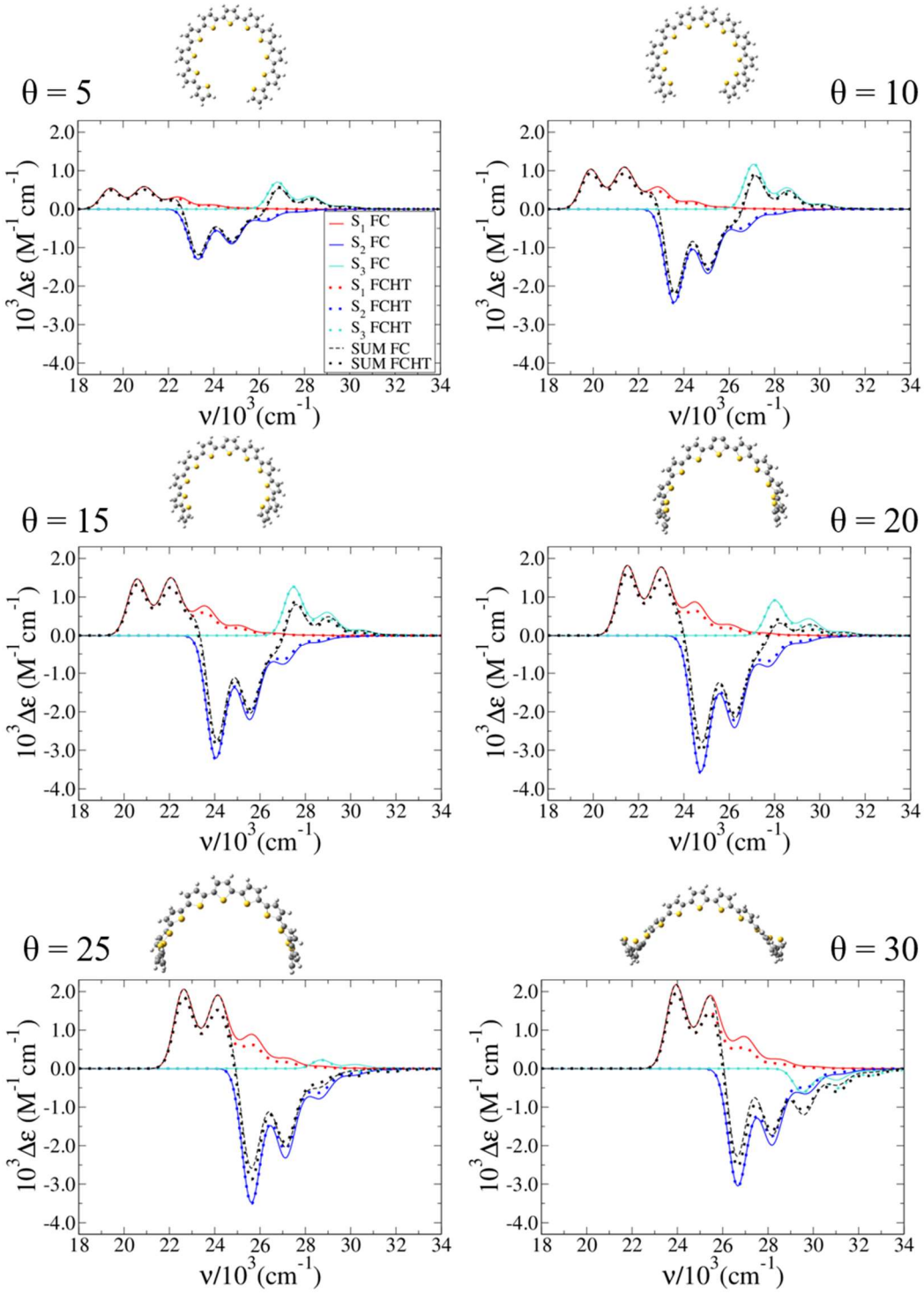

Figure S21. FC and FCHT contribution of S1, S2 and S3 to the ECD spectra computed for the *class II* structure of T_{11} cisoid helices at 0K and broadened with a Gaussian with HWHM=450 cm^{-1} at different torsion angles (considered frozen during the transition).

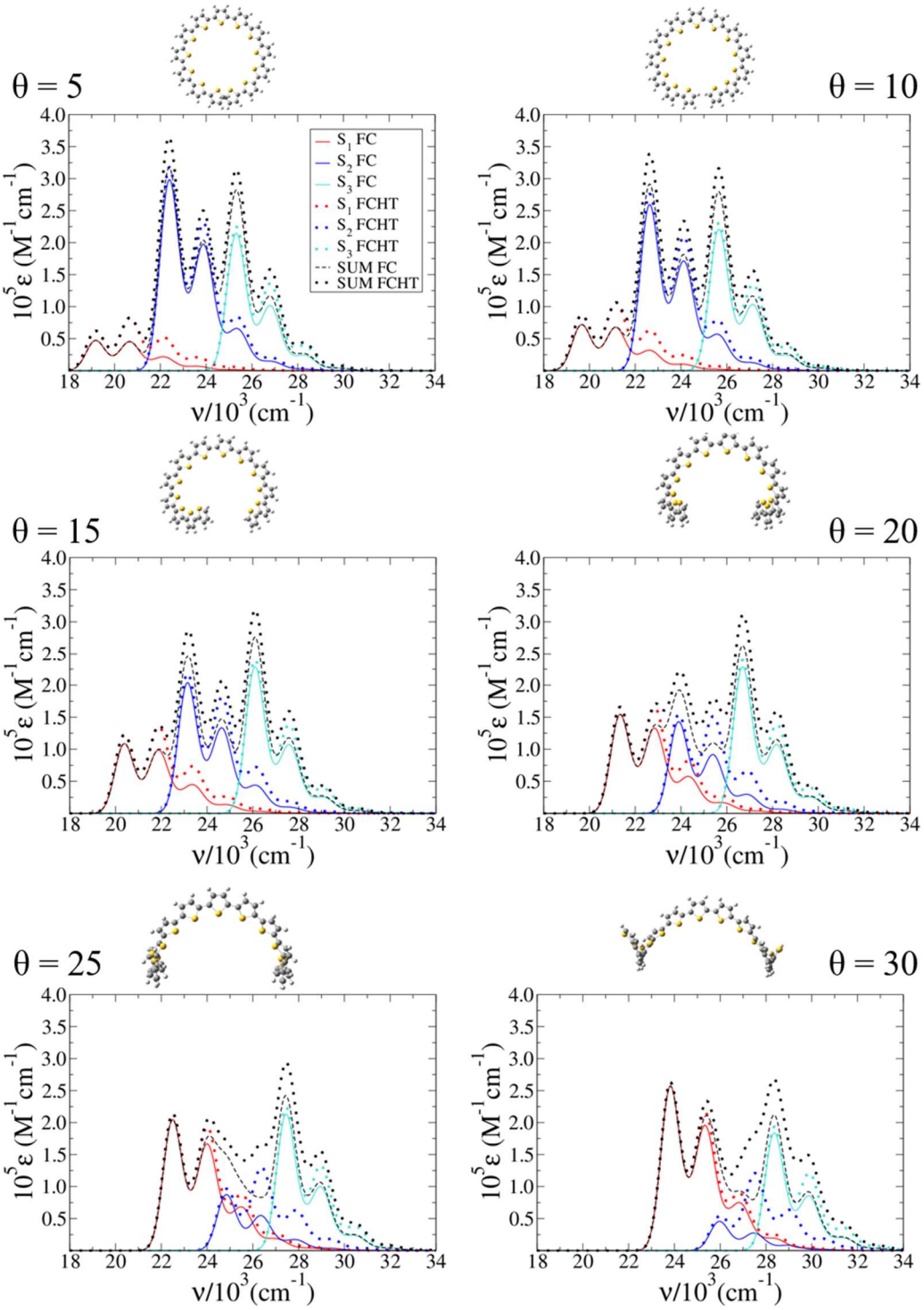

Figure S22. FC and FCHT contribution of S1, S2 and S3 to the absorption spectra computed for the *class II* structure of T_{13} cisoid helices at 0K and broadened with a Gaussian with HWHM=450 cm^{-1} at different torsion angles (considered frozen during the transition).

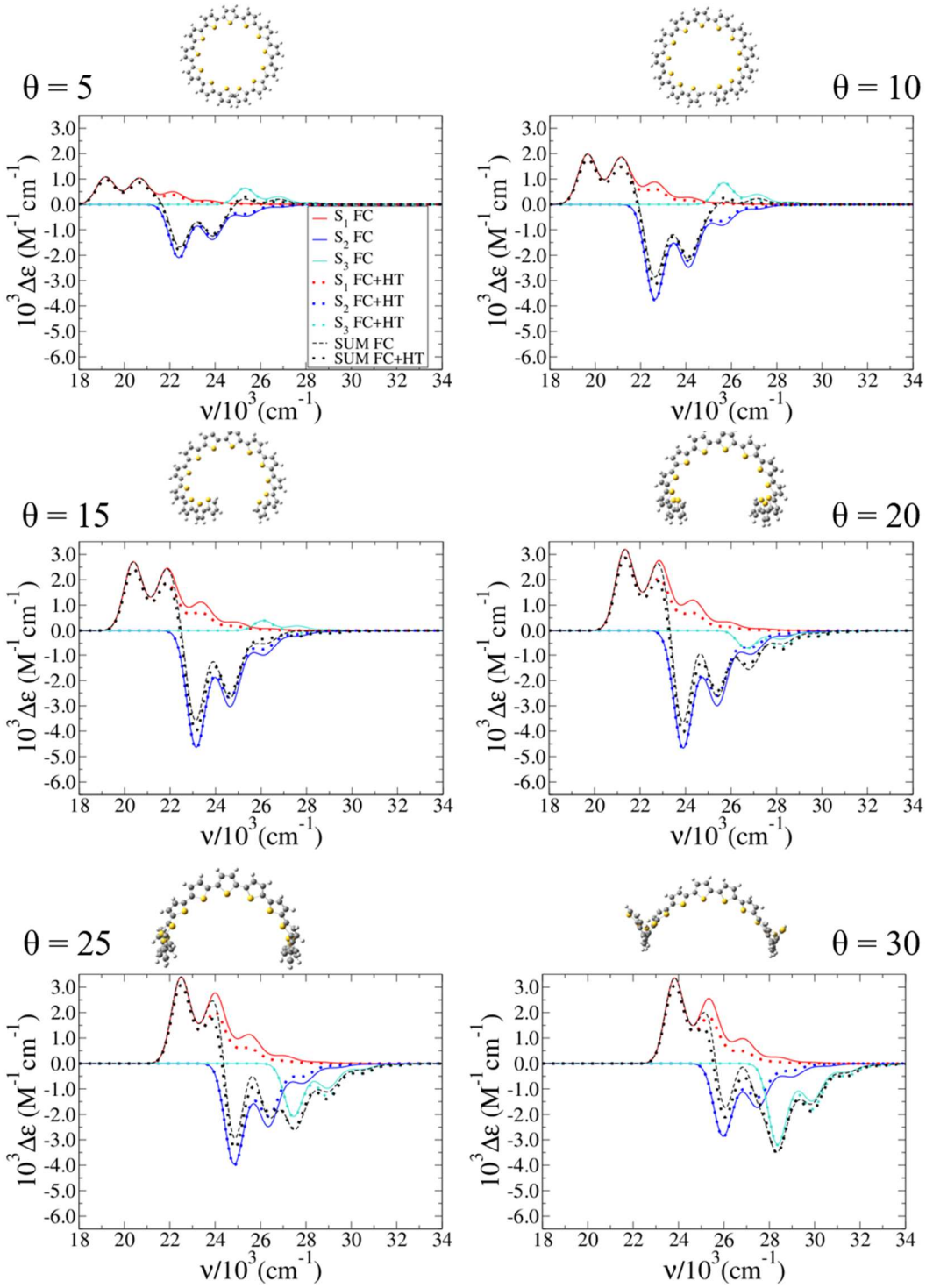

Figure S23. FC and FCHT contribution of S1, S2 and S3 to the ECD spectra computed for the *class II* structure of T_{13} cisoid helices at 0K and broadened with a Gaussian with HWHM=450 cm^{-1} at different torsion angles (considered frozen during the transition).

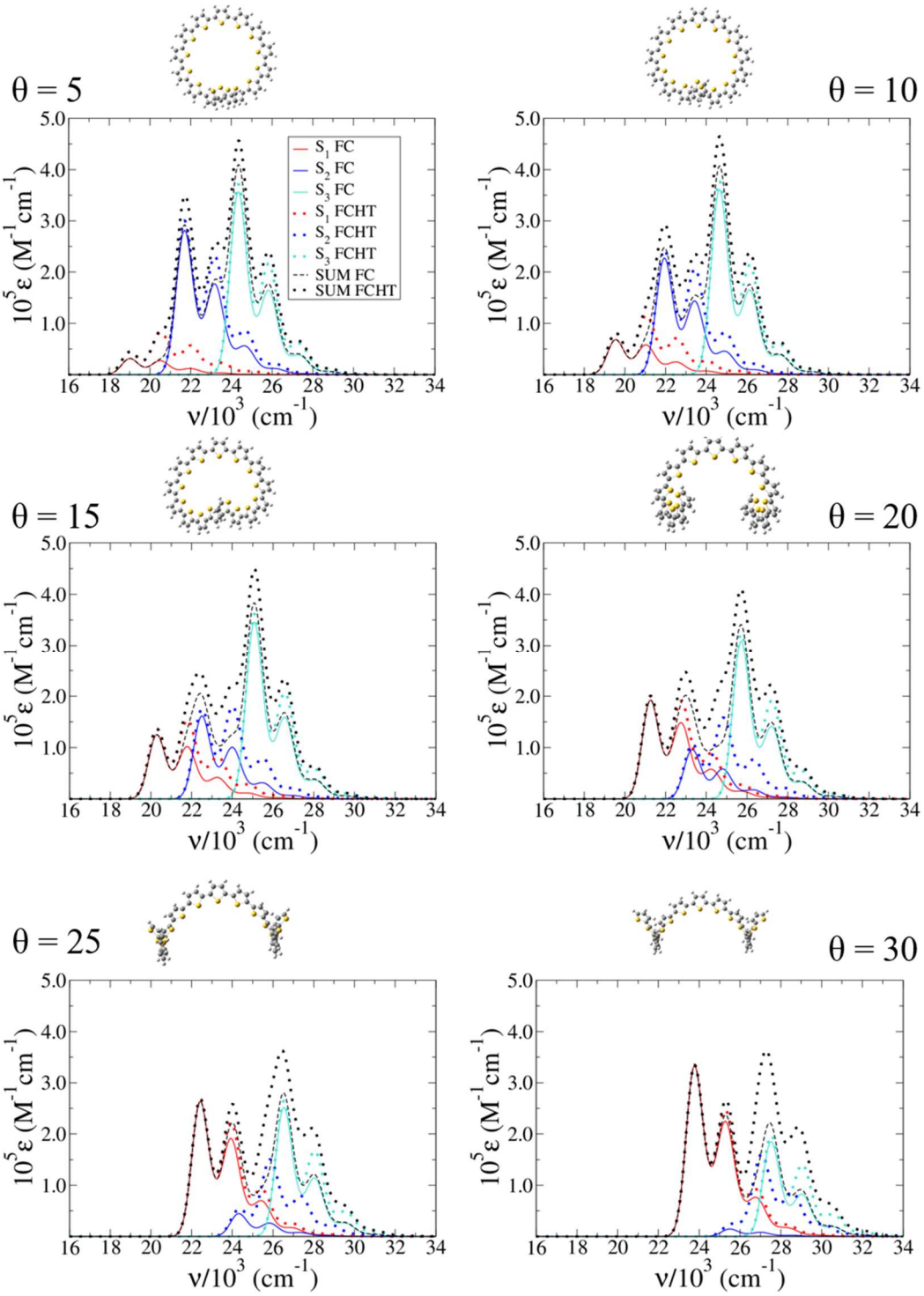

Figure S24. FC and FCHT contribution of S1, S2 and S3 to the absorption spectra computed for the *class II* structure of T_{15} cisoid helices at 0K and broadened with a Gaussian with HWHM=450 cm^{-1} at different torsion angles (considered frozen during the transition).

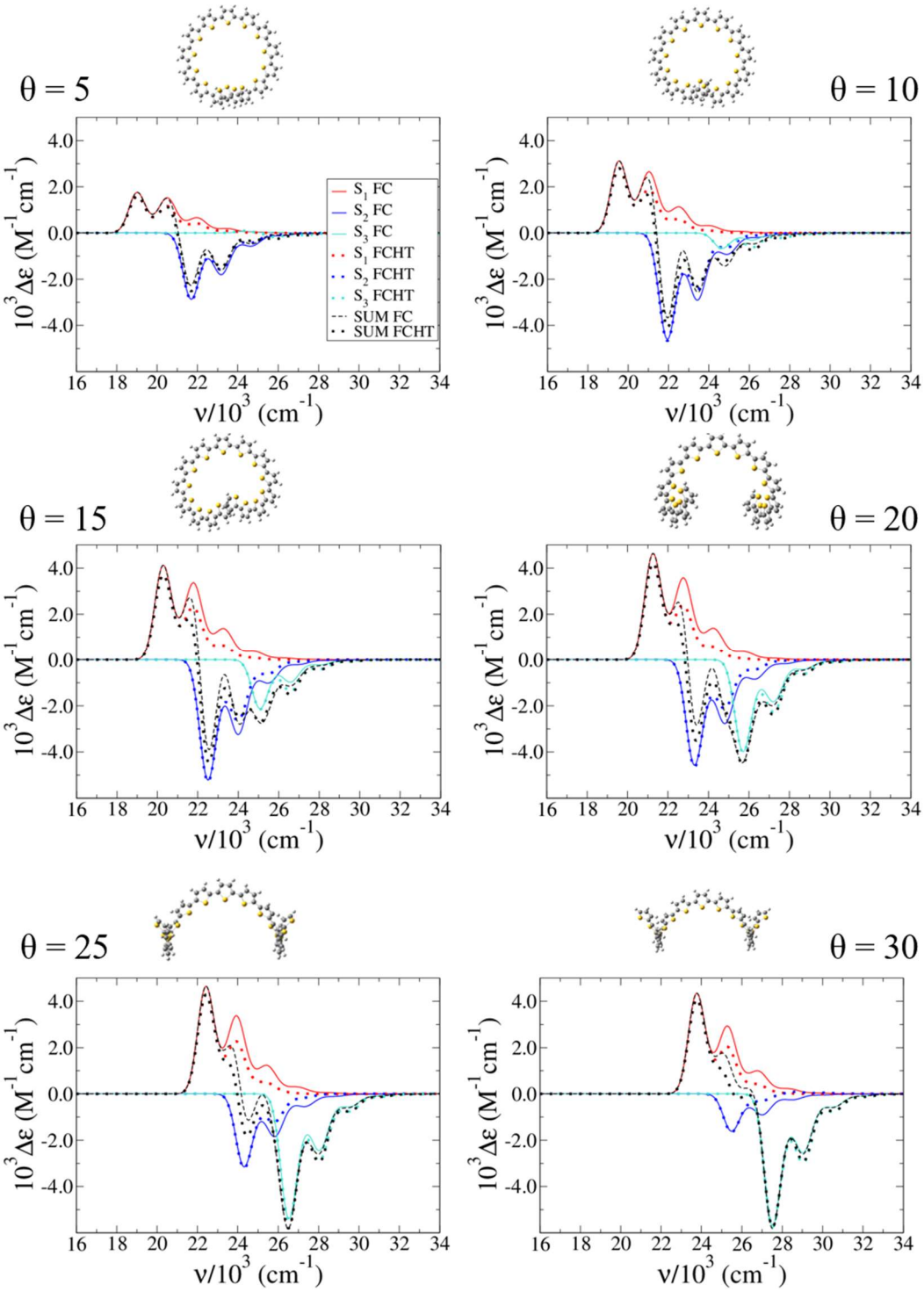

Figure S25. FC and FCHT contribution of S1, S2 and S3 to the ECD spectra computed for the *class II* structure of T_{15} cisoid helices at 0K and broadened with a Gaussian with HWHM=450 cm^{-1} at different torsion angles (considered frozen during the transition).

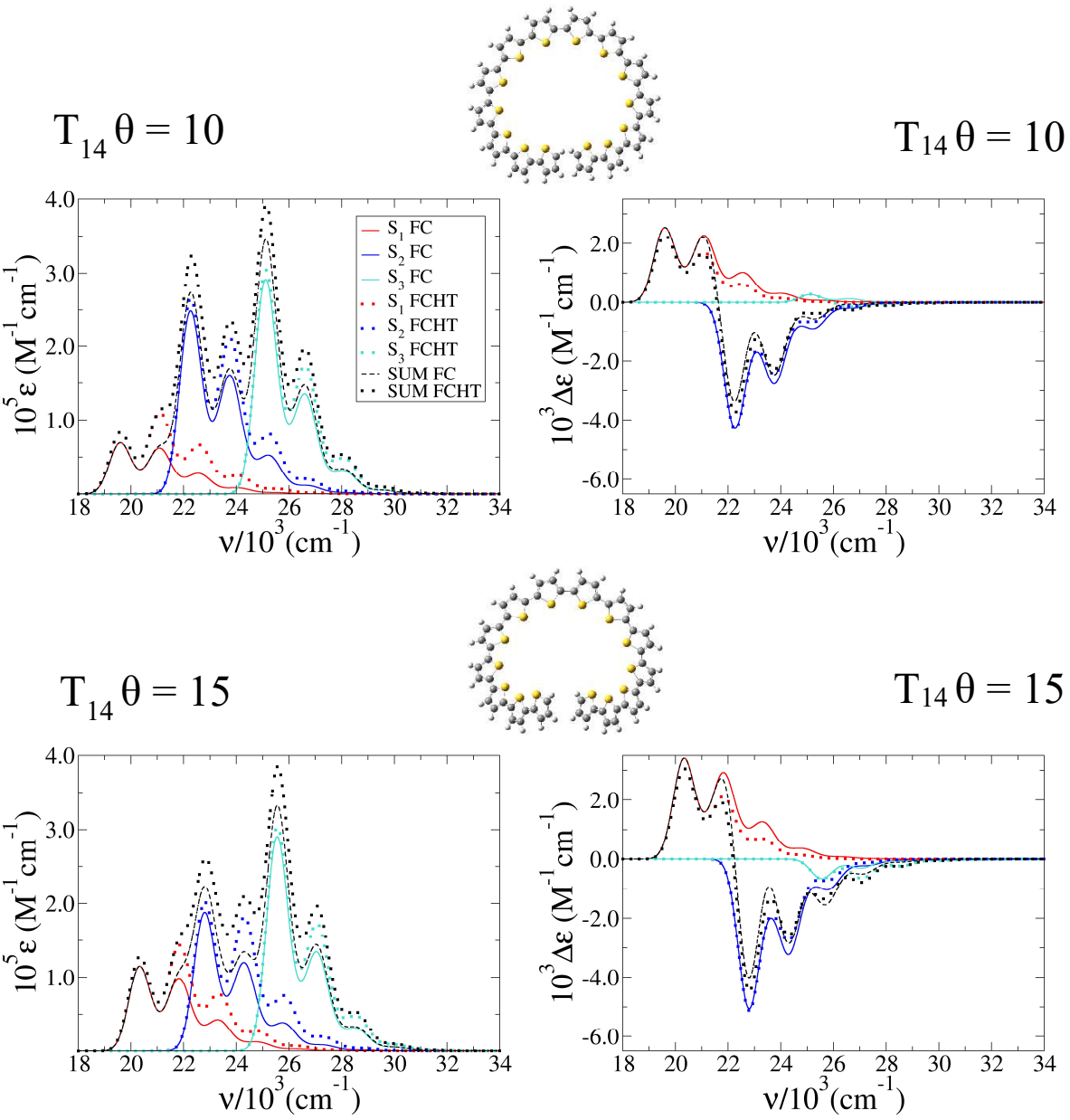

Figure S26. FC and FCHT absorption (left) and ECD (right) spectra computed for the *class II* structure of T_{14} with θ = 10 (top) and θ = 15 (bottom) cisoid helices at 0K and broadened with a Gaussian with HWHM=450 cm^{-1}. Inter-ring torsion angles are considered frozen during the transition.

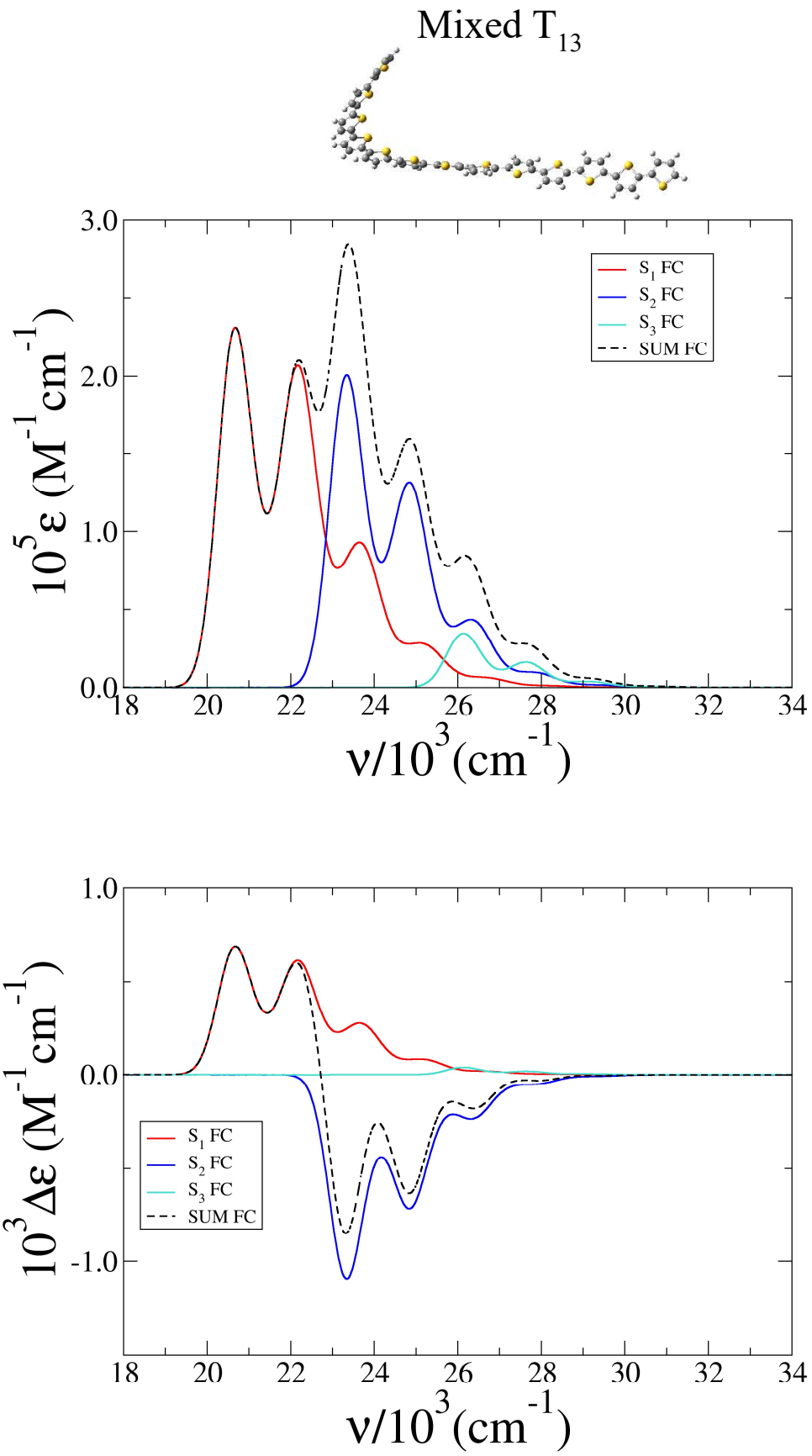

Figure S27. FC absorption (top) and ECD (bottom) spectra computed for the *class II* structure of mixed T_{13} helix at θ=15º, 0K and broadened with a Gaussian with HWHM=450 cm^{-1}. Inter-ring torsion angles are considered frozen during the transition.

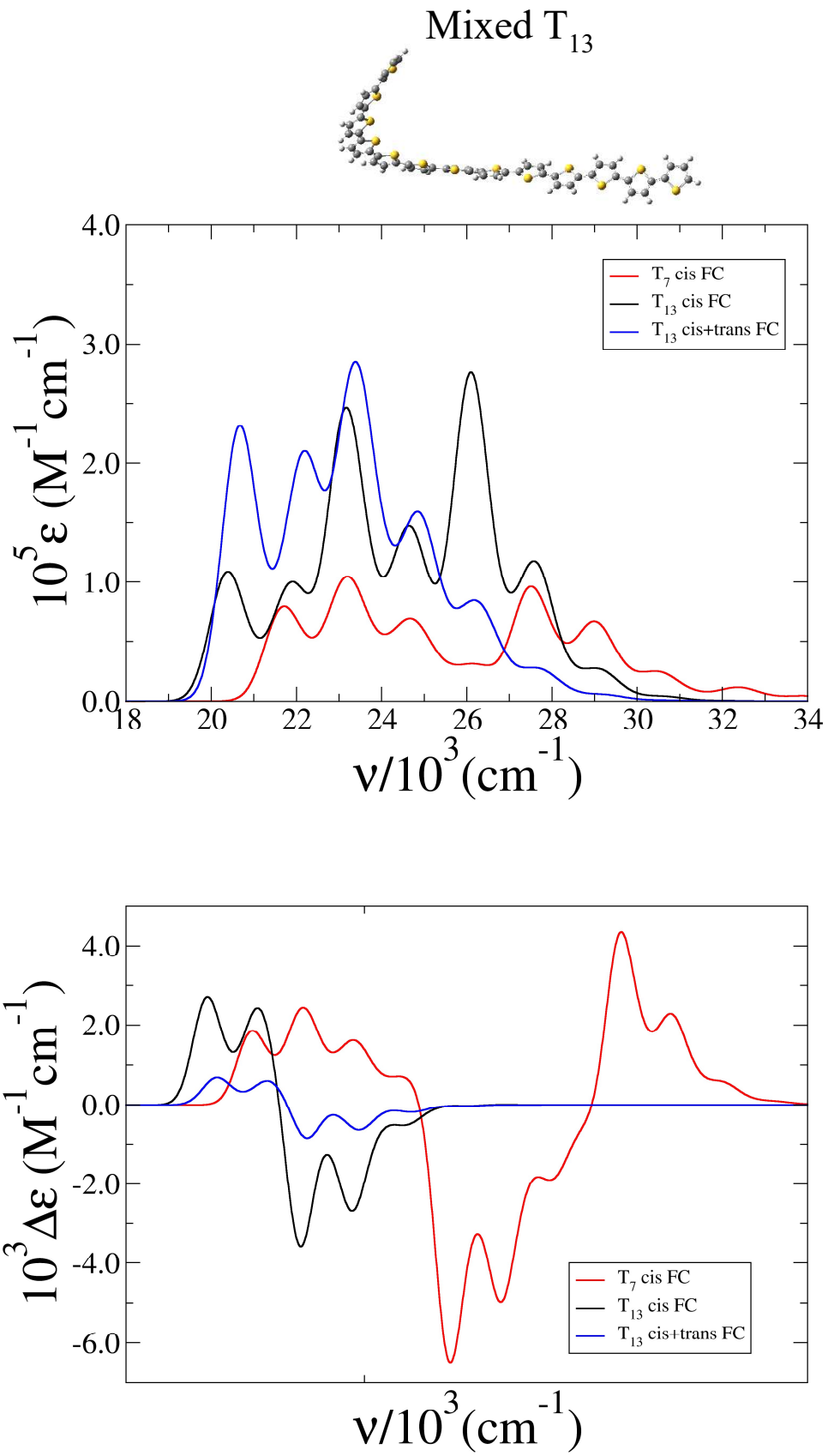

Figure S28. FC absorption (top) and ECD (bottom) spectra computed for the *class II* structures of cisoid T_7, cisoid T_{13} and mixed T_{13} helix. All were computed at θ=15º, 0K and broadened with a Gaussian with HWHM=450 cm^{-1}. Inter-ring torsion angles are considered frozen during the transition.

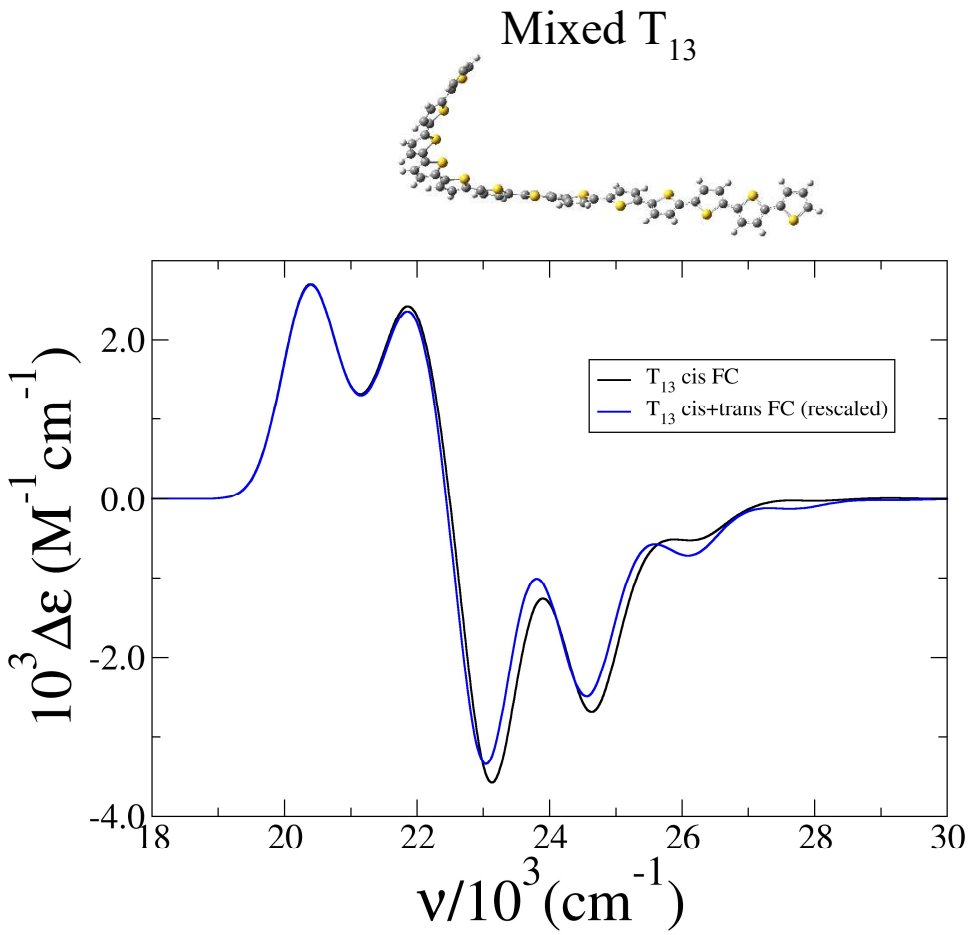

Figure S29. ECD spectra of *class II* structures cisoid T_{13} and mixed T_{13}. The latter was rescaled and shifted to overlap with the first peak of cisoid T_{13}. Both were computed at θ=15º, 0K and broadened with a Gaussian with HWHM=450 cm^{-1}. Inter-ring torsion angles are considered frozen during the transition.

Table S2. Vertical energies (in eV) for the unmethyled (T) and polymethyled (3-methylT) transoid and cisoid T_{13} structures at θ=15º.

	Transoid		Cisoid	
	T_{13}	$(3\text{-methylT})_{13}$	T_{13}	$(3\text{-methylT})_{13}$
S1	2.7657	2.7176	2.6940	2.6803
S2	3.0409	2.9947	2.9922	2.9669
S3	3.3382	3.2931	3.3247	3.2979

Analysis of Molecular Orbitals and transition densities for T_7 and T_{13}.

The Kohn-Sham Molecular Orbitals (MOs) more involved in the S1-S3 electronic states of T_7 and T_{13} are shown in Figures S30-S33 for *transoid* twisted ribbons and *cisoid* helices of T_7 and T_{13} with θ= 10, 20 and 30 degrees. For θ=20 degrees a more in-depth analysis is performed in Figures S34-S39 and Table S3. The description of S1-S3 transitions in terms of excitations between MOs (reported in Table S3) is pretty similar for both *transoid* and *cisoid* structures. S1 is always a HOMO→ LUMO transition, S2 involves both HOMO → LUMO+1 and HOMO-1 → LUMO and S3 arises from HOMO →LUMO+2, HOMO-1 → LUMO+1 and HOMO-2 → LUMO excitations. Inspection of the Figures S30-S33 show that the shapes of the MOs themselves are very similar; therefore it is not surprising that even the S0 → Sn (n=1,2,3) transition densities look pretty similar for *transoid* and *cisoid* helices. Figures S34-S38 show that transoid structures mostly extend in the direction of the non-total symmetric Y axis. On the contrary, cisoid helices extend along all the three axes (Z is the total symmetric one). The X, Y and Z Cartesian components of the electric transition moment associated to these transitions can be computed by the integral of the transition densities ($\rho_{0n}(X,Y,Z)$) multiplied by the value of the corresponding coordinate $\mu_{0n}(X) \propto \int X\rho_{0n}(X,Y,Z)d\mathbf{r}$, $\mu_{0n}(Y) \propto \int Y\rho_{0n}(X,Y,Z)d\mathbf{r}$, $\mu_{0n}(Z) \propto \int Z\rho_{0n}(X,Y,Z)d\mathbf{r}$. The different spatial arrangments of *transoid* and *cisoid* structures have a deep impact on these integrands. Consider T_7: S1 state belongs to B irreps. Accordingly, it can have X and Y components of the transition dipole. Due to the almost linear structure of the transoid twisted ribbon, oriented along Y, the transition is almost completely Y-polarized. $\mu_{01}(Y)$ is the largest component also for the cisoid structure but in this case also $\mu_{01}(X)$ is significant. Notice, on the contrary, that $Z\rho_{01}(X,Y,Z)$ is an odd function and therefore its integral is zero. The same is true for $X\rho_{02}(X,Y,Z)$ and $Y\rho_{02}(X,Y,Z)$ of both transoid and cisoid structures, as expected since in both cases, S2 belongs to the A irreps. However, $Z\rho_{02}(X,Y,Z)$ shows a large difference in the two cases. In fact cisoid helix is much more elongated along the Z axis so that the same transition density is actually more stretched along such axis in cisoid than in transoid structures. Multiplication by "Z" therefore enhances the contributions of the atoms at large positive and negative Z values, giving a trasition dipole 70-80 times larger in cisoid helix. The same phenomenon occurs for S1 and S2 of cisoid and transoid T_{13}. In the cisoid arrangement of T_{13} however, also S3 (B symmetry) acquires a remarkable transition dipole. Interestingly, even if $Y\rho_{03}(X,Y,Z)$ shows bigger positive and negative lobes than $X\rho_{03}(X,Y,Z)$ the X component of the transition dipole is

much larger than the Y one. This result can be rationalized noticing that while in $Y\rho_{03}(X,Y,Z)$ there is an alternation of violet (negative) and cyan (positive) lobes, in $X\rho_{03}(X,Y,Z)$ the negative lobes largely dominate, and in fact $\mu_{03}(X)$ is large and negative. Interestingly the plot for cisoid T_7 and T_{13} shows that the transition densities of the former multiplied by X and Y show an alternation of positive and negative lobes, so that their integral is small. With respect to T_7, the T_{13} structure exhibits left and right wings that elongate in X and Y directions. Its transition density multiplied by X is mainly negative on these extreme parts of the molecule (absent in T_7) and this explains why S3 acquires a strong negative X component of the transition dipole that is not seen in T_7 (Figure S39).

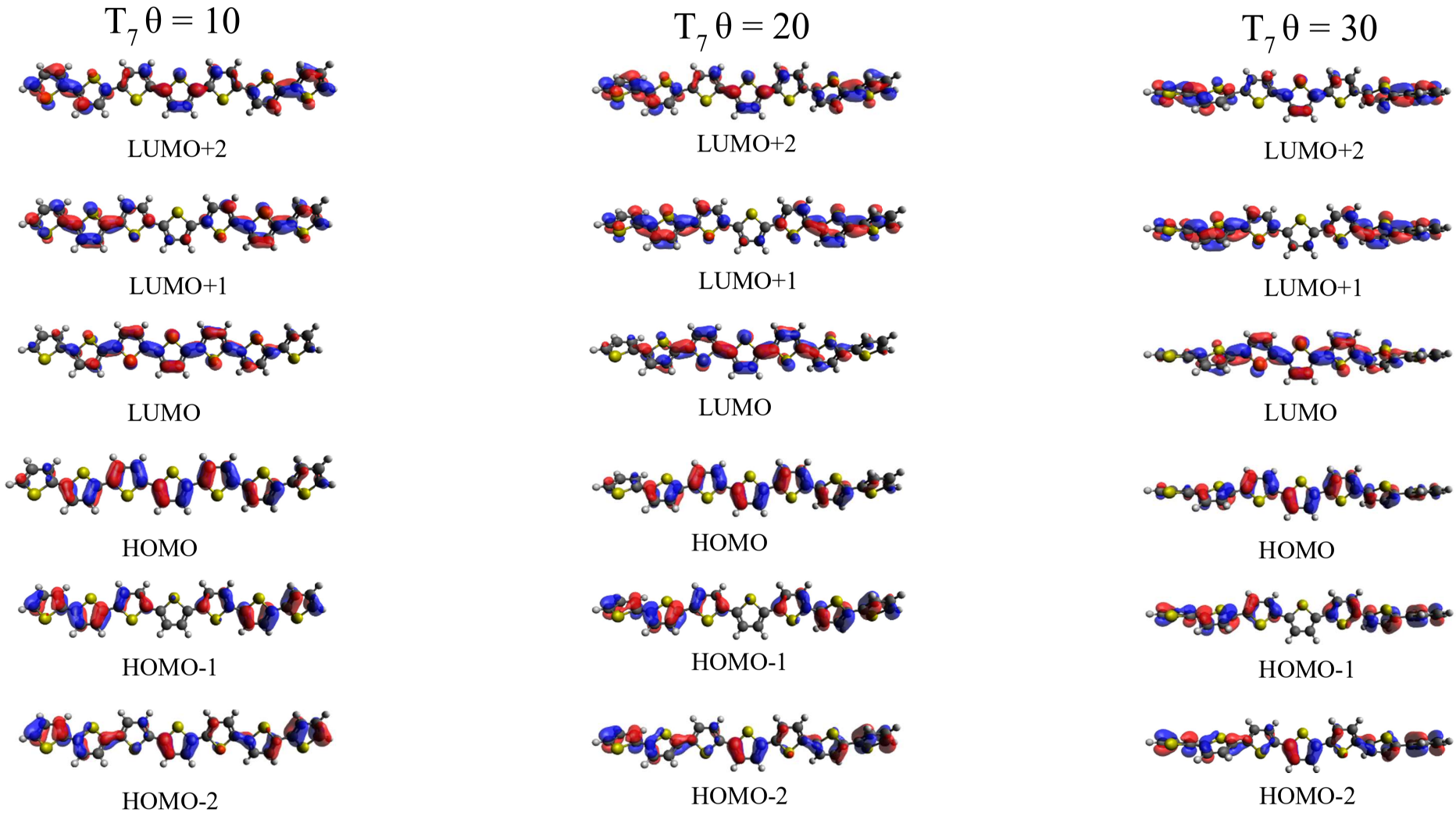

Figure S30. Transoid T_7 Main orbitals involved in the S1 (HOMO -> LUMO), S2 (HOMO -> LUMO +1, HOMO-1, LUMO) and S3 (HOMO -> LUMO+2, HOMO-1 -> LUMO, HOMO-2 -> LUMO) transitions at different torsion angles. Isovalue = 0.03.

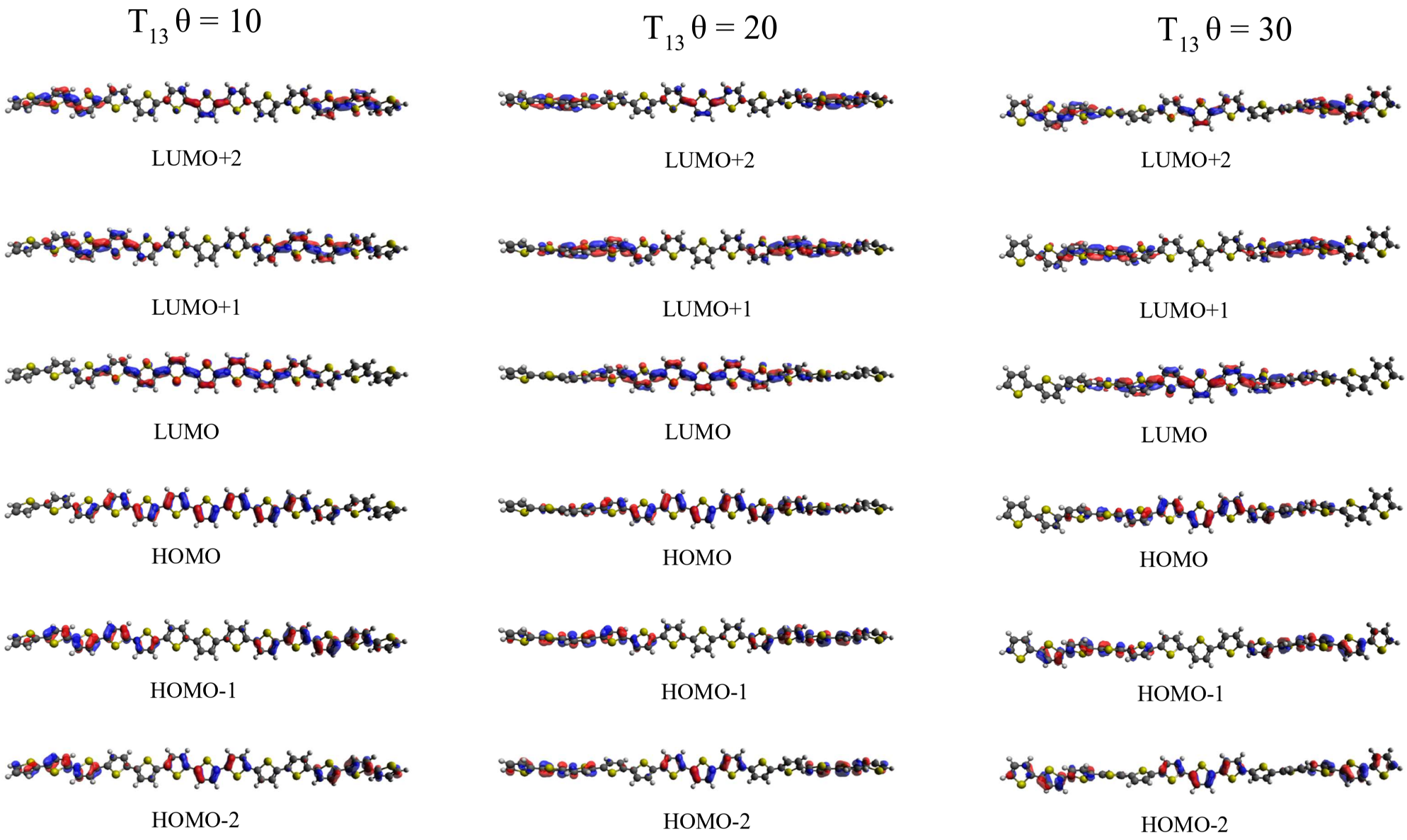

Figure S31. Transoid T_{13} Main orbitals involved in the S1 (HOMO -> LUMO, HOMO-1 -> LUMO+1), S2 (HOMO -> LUMO +1, HOMO-1, LUMO) and S3 (HOMO -> LUMO+2, HOMO-1 -> LUMO, HOMO-2 -> LUMO) transitions at different torsion angles. Isovalue = 0.03

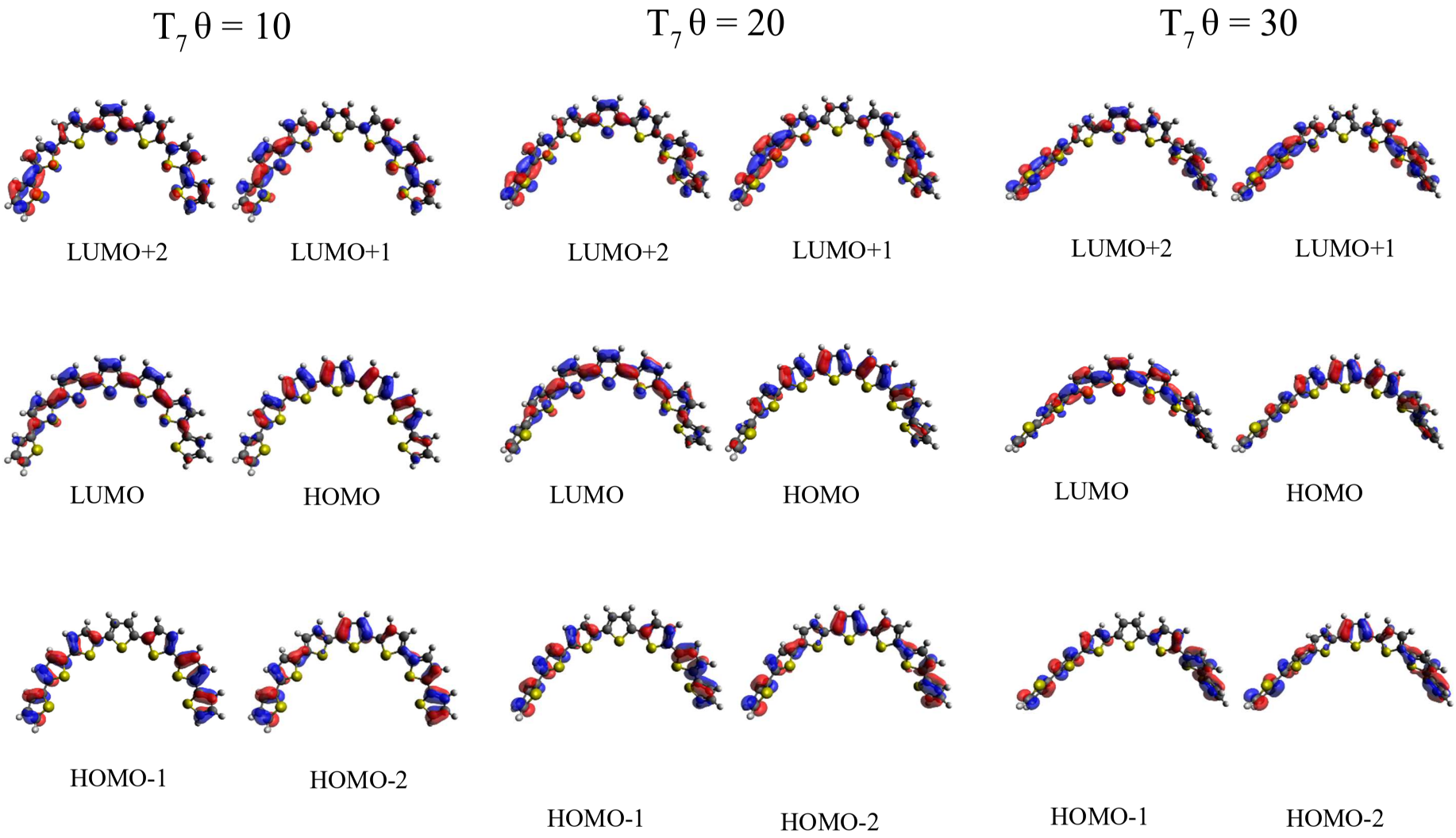

Figure S32. Cisoid T_7 Main orbitals involved in the S1 (HOMO -> LUMO), S2 (HOMO -> LUMO +1, HOMO-1->LUMO) and S3 (HOMO -> LUMO+2, HOMO-1 -> LUMO, HOMO-2 -> LUMO) transitions at different torsion angles. Isovalue = 0.03.

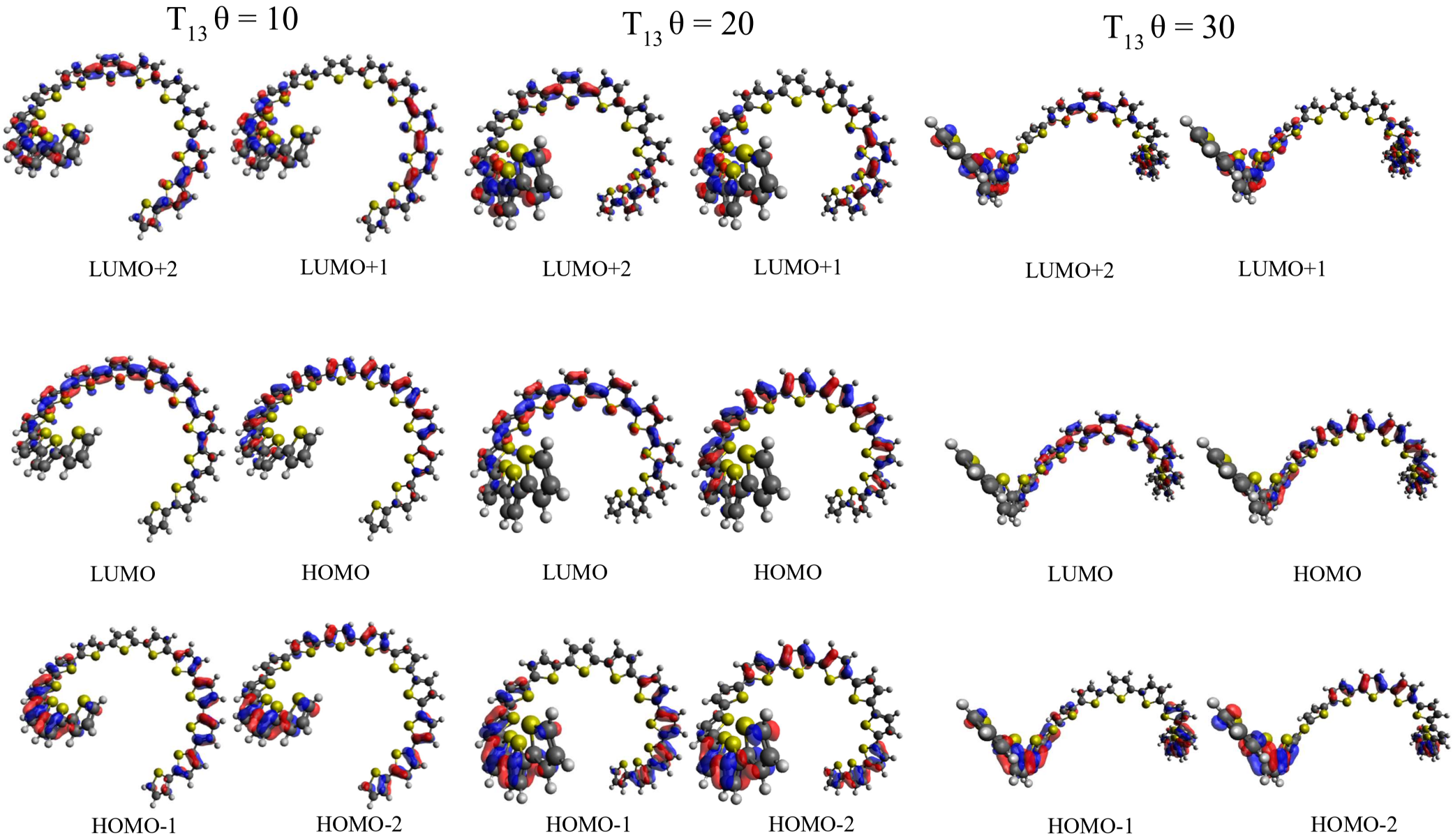

Figure S33. Cisoid T_{13} Main orbitals involved in the S1 (HOMO -> LUMO, HOMO-1 -> LUMO+1), S2 (HOMO -> LUMO +1, HOMO-1->LUMO) and S3 (HOMO -> LUMO+2, HOMO-1 -> LUMO, HOMO-2 -> LUMO) transitions at different torsion angles. Isovalue = 0.03

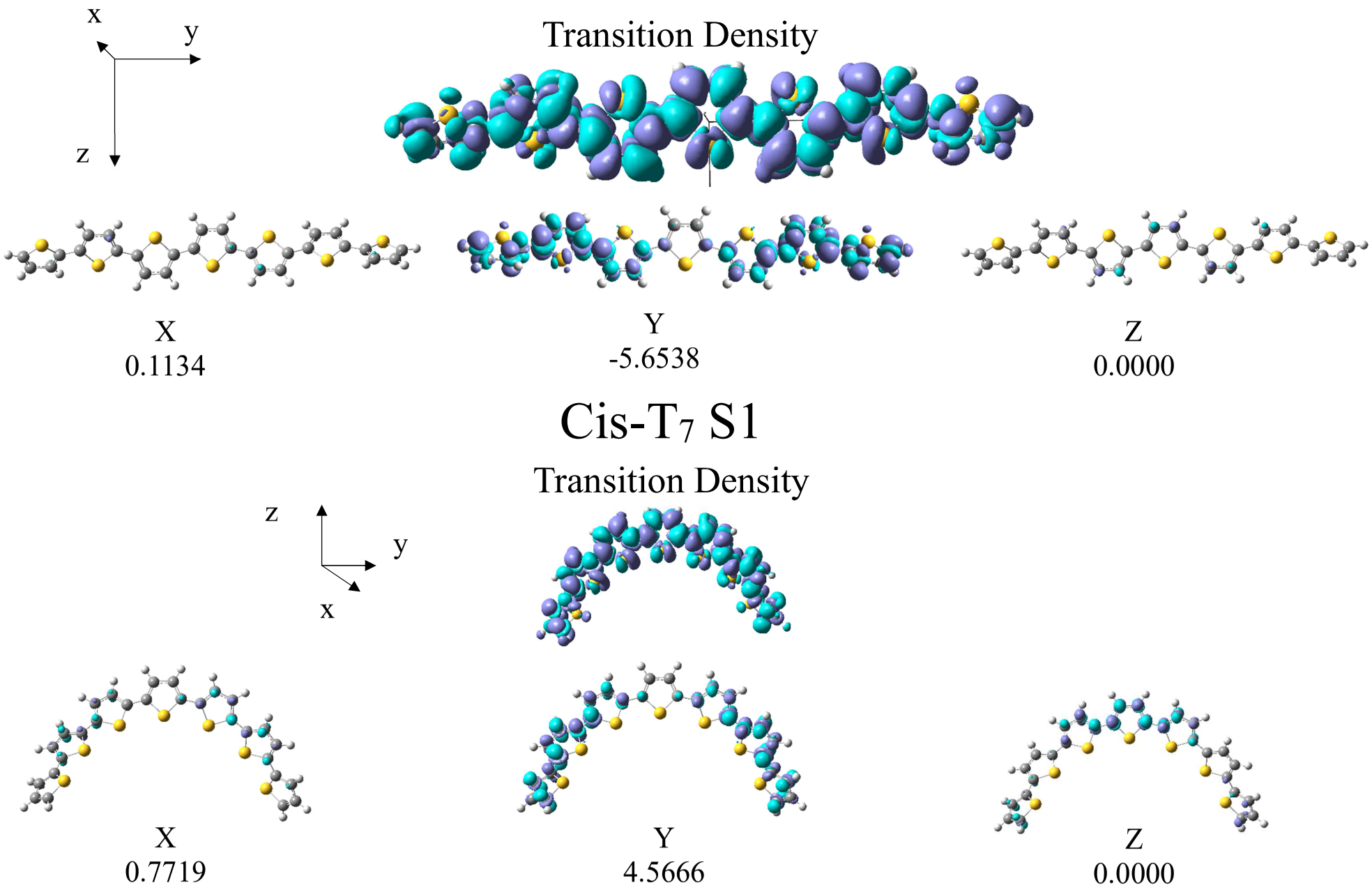

Figure S34. T_7 at θ = 20º : Plot of the transition densities involved in the S1 (HOMO -> LUMO) and of their product by the Cartesian coordinates . The components of the transition electric dipole moment are shown below. Isovalue = 0.0004 for all plots except for the transition densities of transoid T_7 multiplied by X, Y and Z, whose isovalue is 0.00004.

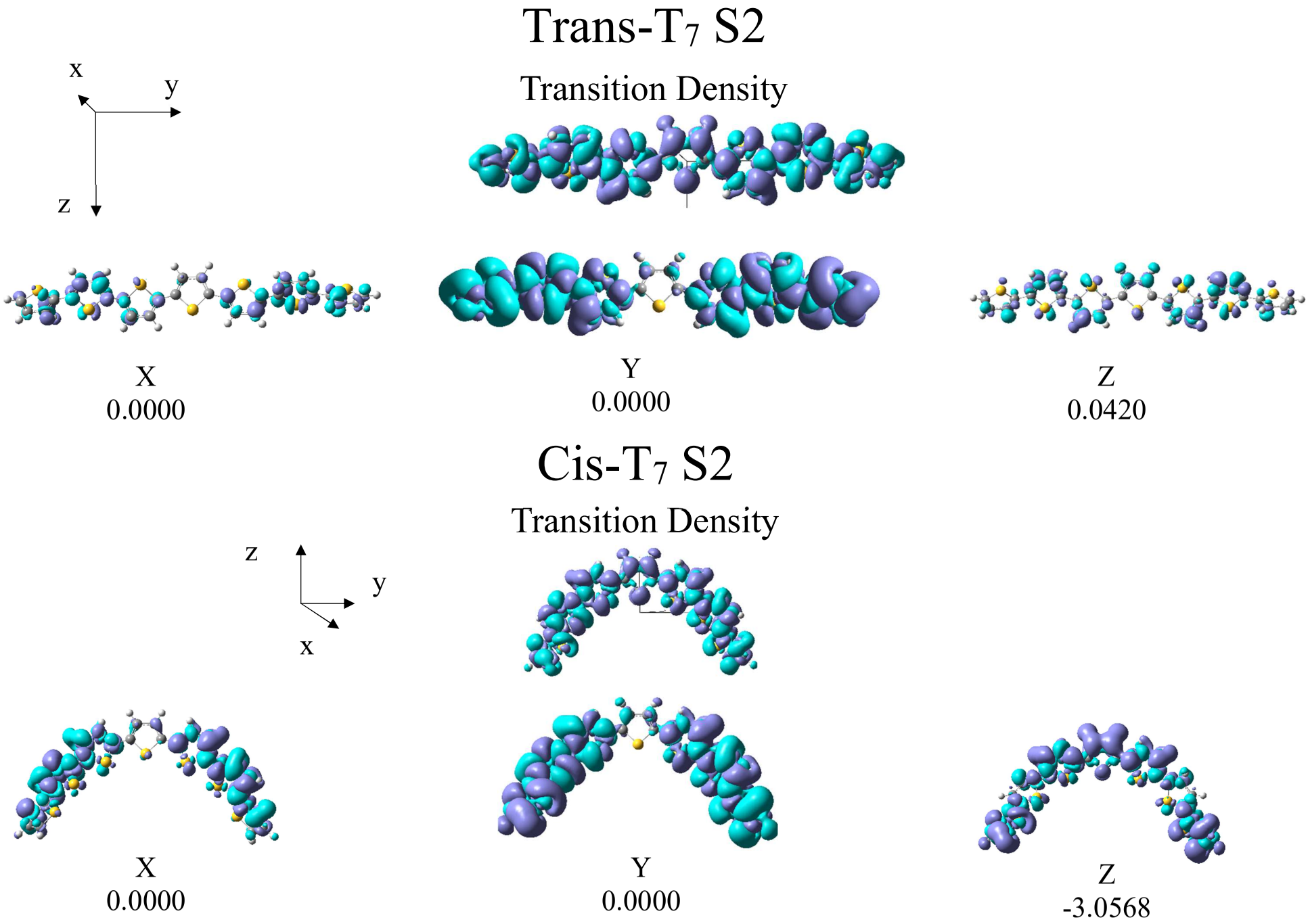

Figure S35. T_7 at θ = 20º : Plot of the transition densities involved in the S2 (HOMO -> LUMO+1, HOMO-1 -> LUMO) and of their product by the Cartesian coordinates . The components of the transition electric dipole moment are shown below. Isovalue = 0.0004 for all plots except for the transition densities of transoid T_7 multiplied by X, Y and Z, whose isovalue is 0.00004.

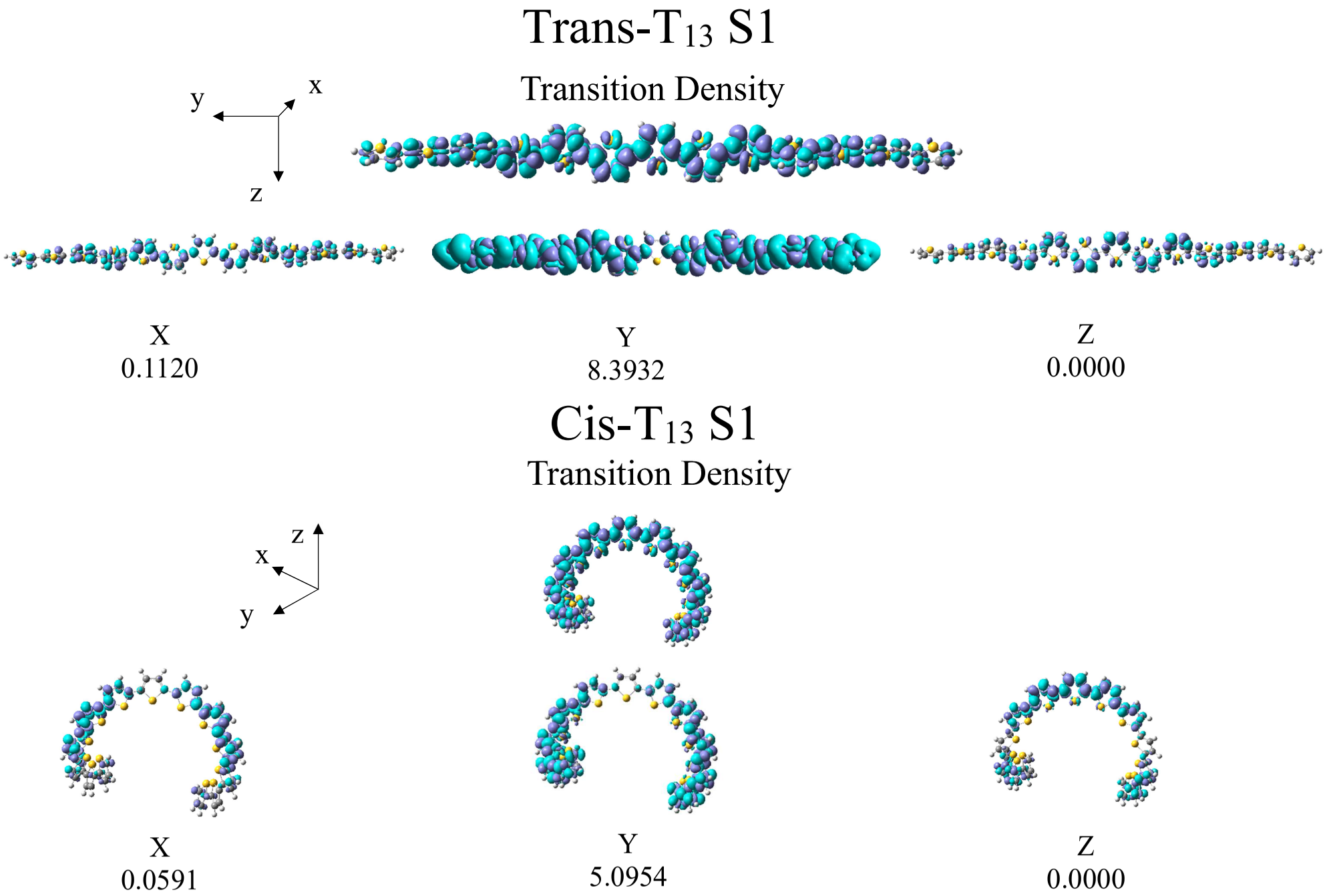

Figure S36. T_{13} at θ = 20º : Plot of the transition densities involved in the S1 (HOMO -> LUMO) and of their product by the Cartesian coordinates . The components of the transition electric dipole moment are shown below. Isovalue = 0.0004 for all plots except for the transition densities of transoid T_{13} multiplied by X, Y and Z, whose isovalue is 0.00004.

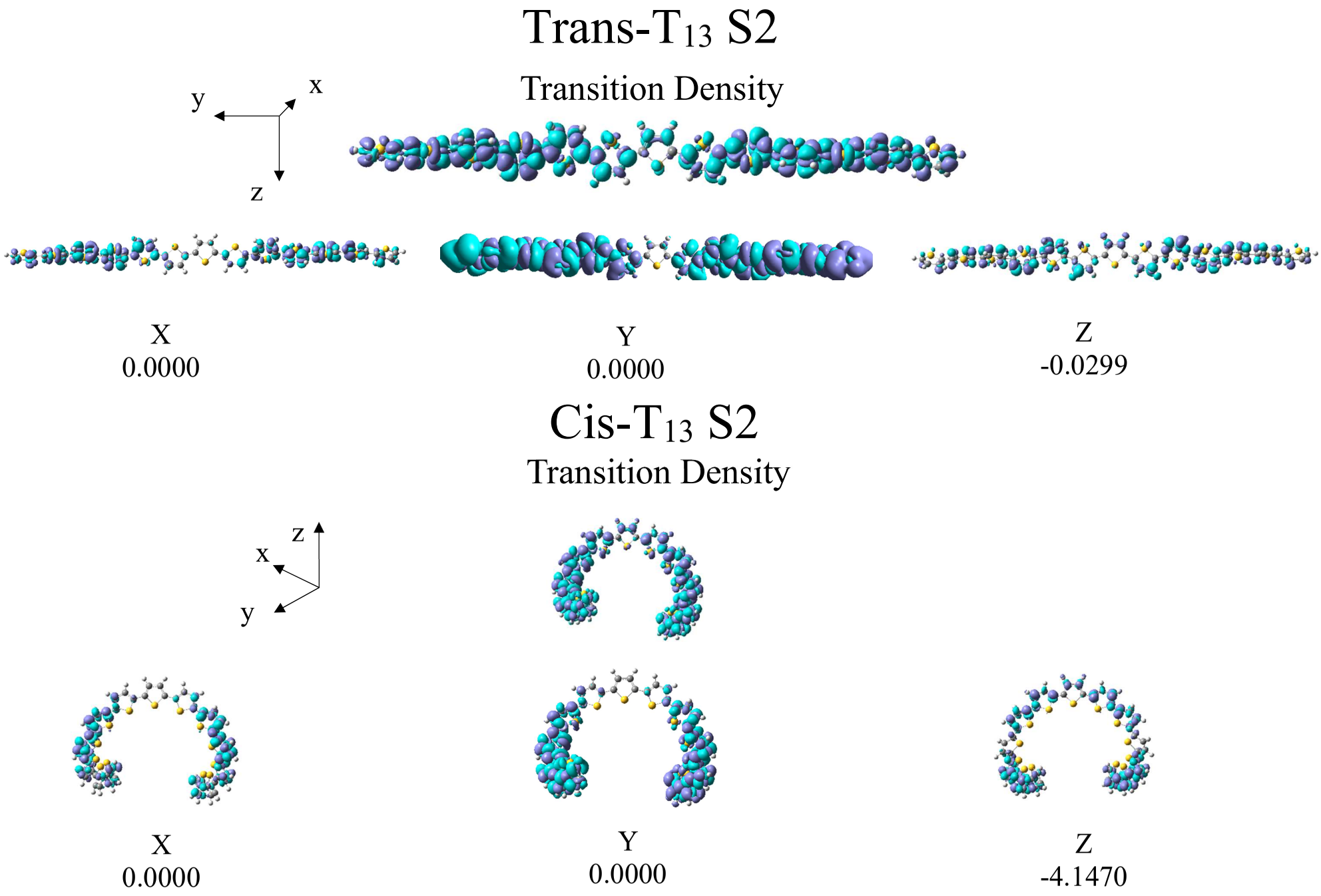

Figure S37. T_{13} at θ = 20º : Plot of the transition densities involved in the S2 (HOMO -> LUMO+1, HOMO-1 -> LUMO) and of their product by the Cartesian coordinates . The components of the transition electric dipole moment are shown below. Isovalue = 0.0004 for all plots except for the transition densities of transoid T_{13} multiplied by X, Y and Z, whose isovalue is 0.00004.

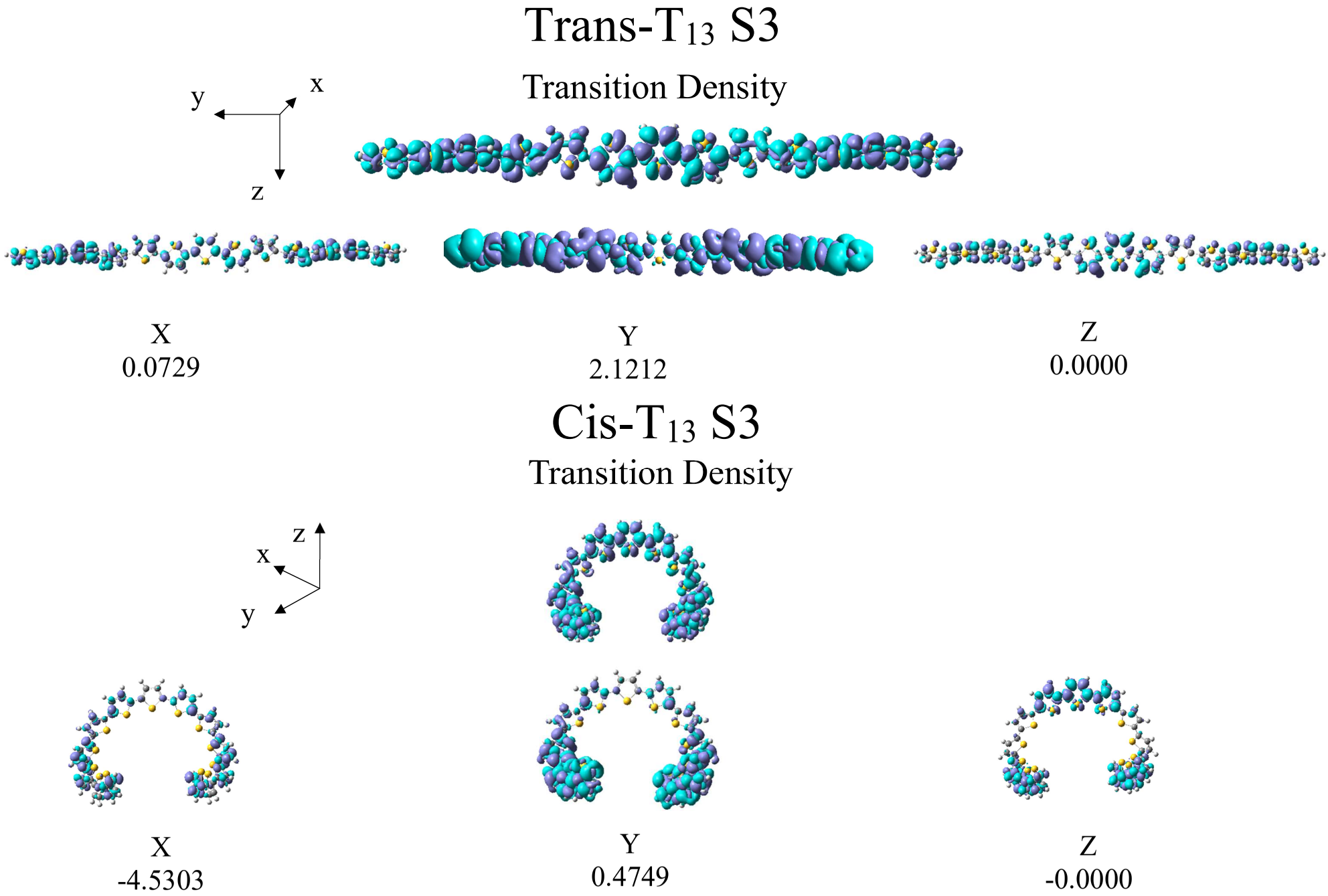

Figure S38. T_{13} at θ = 20º : Plot of the transition densities involved in the S3 (HOMO -> LUMO+2, HOMO-1 -> LUMO+1, HOMO-2 -> LUMO) and of their product by the Cartesian coordinates . The components of the transition electric dipole moment are shown below. Isovalue = 0.0004 for all plots except for the transition densities of transoid T_{13} multiplied by X, Y and Z, whose isovalue is 0.00004.

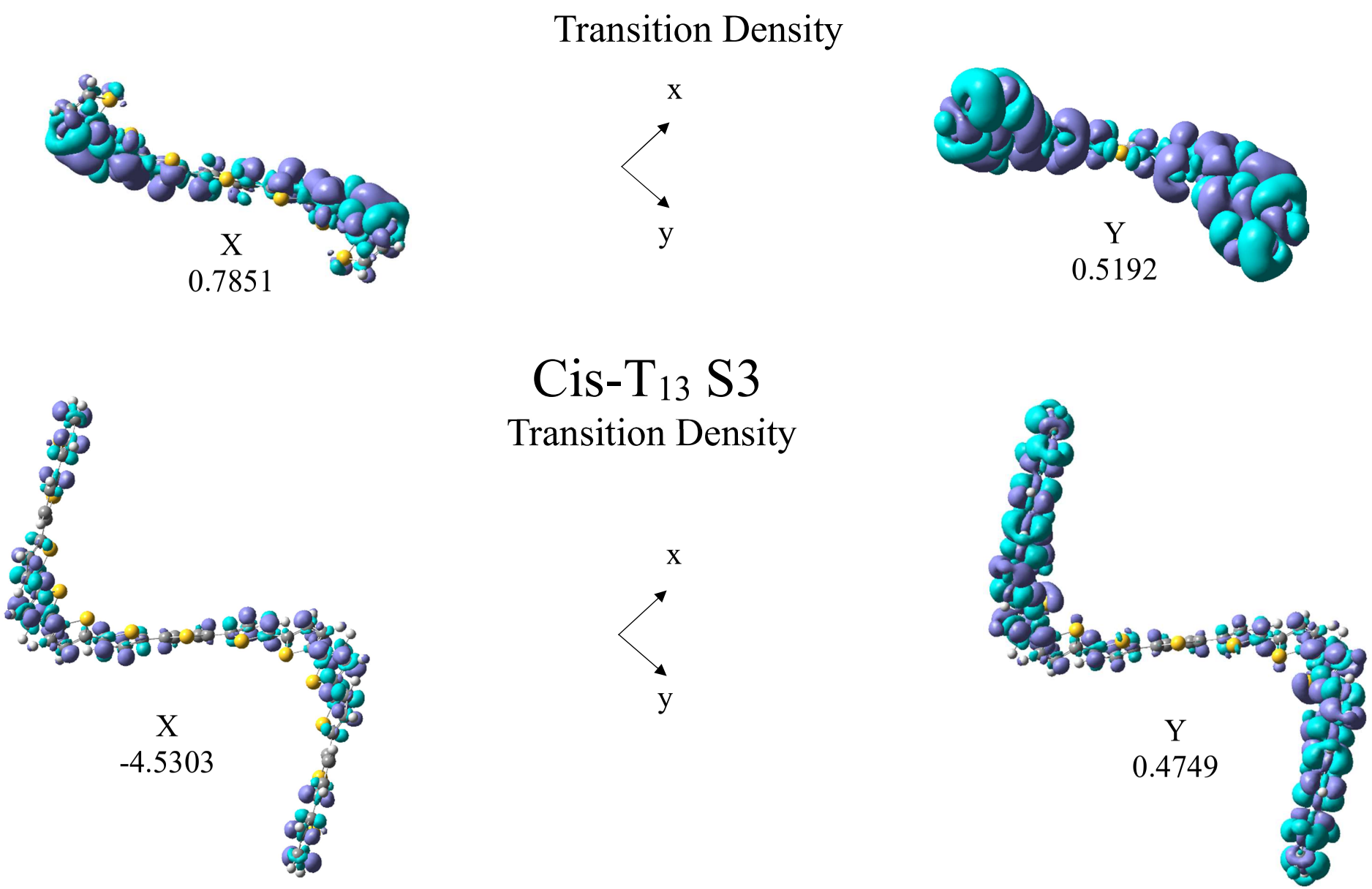

Figure S39. T_7 and T_{13} at θ=20º : Plot of the transition densities multiplied by the X and Y Cartesian coordinates involved in S3 (HOMO -> LUMO+2, HOMO-1 -> LUMO+1, HOMO-2-> LUMO). The components of the transition electric dipole moment are shown below. Isovalue = 0.00004 for T_7 and 0.0004 for T_{13}. The components of the transition electric dipole moment are shown below.

Table S3. T_7 and T_{13} data for the three lowest energy excited states at $\theta = 20^{o}$. (a) Composition of the main transitions in terms of the molecular orbitals involved. (b) Vertical transition energies in eV. (c) Oscillator strengths. (d) Rotatory strengths.

(a)

Excited State	Composition
S1	HOMO -> LUMO
S2	HOMO -> LUMO+1, HOMO-1 -> LUMO
S3	HOMO -> LUMO+2, HOMO-1 -> LUMO+1, HOMO-2 -> LUMO

(b) Vertical Transition Energy (eV)

	T_7		T_{13}	
	Cisoid	Transoid	Cisoid	Transoid
S1	3.0275	3.0735	2.8060	2.8664
S2	3.6187	3.6179	3.0839	3.1272
S3	4.1718	4.1298	3.3996	3.4097

(c) Oscillator Strength

	T_7		T_{13}	
	Cisoid	Transoid	Cisoid	Transoid
S1	1.591	2.4079	1.7851	4.948
S2	0.8284	0.0002	1.2994	0.0001
S3	0.0969	0.1863	1.7282	0.3763

(d) Rotatory Strength (10^{-40} cgs)

	T_7		T_{13}	
	Cisoid	Transoid	Cisoid	Transoid
S1	1018.8830	-228.5557	8705.1499	-450.4941
S2	-1631.8471	-3.5887	-9073.8208	1.8572
S3	697.0429	-8.0884	-1053.0201	-40.4677